Design and Evaluation of a Biomimetic Agonist-Antagonist Active Knee Prosthesis

by

Ernesto Carlos Martínez-Villalpando

B.S., Electrical and Digital Systems Engineering
Universidad Panamericana campus Bonaterra, 2001

S.M., Media Arts and Sciences
Massachusetts Institute of Technology, 2006

Thesis submitted to the Program in Media Arts and Sciences,
School of Architecture and Planning,
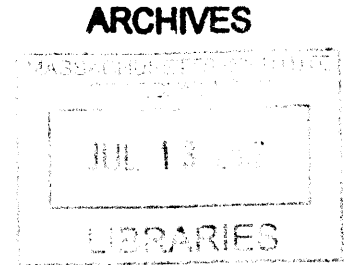in partial fulfillment of the requirements for the degree of

Doctor of Philosophy

at the

MASSACHUSETTS INSTITUTE OF TECHNOLOGY

June 2012

Author: ....
Program in Media Arts and Sciences
March 30th , 2012

Certified by: ....
Hugh Herr, Ph.D.
Associate Professor of Media Arts and Sciences
and Health Sciences and Technology

Accepted by: ....
Mitchel Resnick, Ph.D.
Chair, Department Committee of Graduate Studies
Program in Media Arts and Sciences

Design and Evaluation of a Biomimetic Agonist-Antagonist Active Knee Prosthesis
by
Ernesto Carlos Martínez Villalpando

Thesis submitted to the Program in Media Arts and Sciences,
School of Architecture and Planning on March 30th, 2012
in partial fulfillment of the requirements for the degree of
Doctor of Philosophy

Abstract

The loss of a limb is extremely debilitating. Unfortunately, today's assistive technologies are still far from providing fully functional artificial limb replacements. Although lower extremity prostheses are currently better able to give assistance than their upper-extremity counterparts, important locomotion problems still remain for leg amputees. Instability, gait asymmetry, decreased walking speeds and high metabolic energy costs are some of the main challenges requiring the development of a new kind of prosthetic device. These challenges point to the need for highly versatile, fully integrated lower-extremity powered prostheses that can replicate the biological behavior of the intact human leg.

This thesis presents the design and evaluation of a novel biomimetic active knee prosthesis capable of emulating intact knee biomechanics during level-ground walking. The knee design is motivated by a mono-articular prosthetic knee model comprised of a variable damper and two series-elastic clutch units spanning the knee joint. The powered knee system is comprised of two series-elastic actuators positioned in parallel in an agonist-antagonist configuration. This investigation hypothesizes that the biomimetic active-knee prosthesis, with a variable impedance control, can improve unilateral transfemoral amputee locomotion in level-ground walking, reducing the metabolic cost of walking at self-selected speeds.

To evaluate this hypothesis, a preliminary study investigated the clinical impact of the active knee prosthesis on the metabolic cost of walking of four unilateral above-knee amputees. This preliminary study compared the antagonistic active knee prosthesis with subjects' prescribed knee prostheses. The subjects' prescribed prostheses encompass four of the leading prosthetic knee technologies commercially available, including passive and electronically controlled variable-damping prosthetic systems. Use of the novel biomimetic active knee prosthesis resulted in a metabolic cost reduction for all four subjects by an average of 5.8%. Kinematic and kinetic analyses indicate that the active knee can increase self-selected walking speed in addition to reducing upper body vertical displacement during walking by an average of 16%. The results of this investigation report for the first time a metabolic cost reduction when walking with a prosthetic system comprised of an electrically powered active knee and passive foot-ankle prostheses, as compared to walking with a conventional transfemoral prosthesis.

With this work I aim to advance the field of biomechatronics, contributing to the development of integral assistive technologies that adapt to the needs of the physically challenged.

Thesis Supervisor: Hugh Herr, Ph.D.
Associate Professor of Media Arts and Sciences,
and Health Sciences and Technology

Design and Evaluation of a Biomimetic Agonist-Antagonist Active Knee Prosthesis

by

Ernesto Carlos Martínez-Villalpando

Thesis submitted to the Program in Media Arts and Sciences,
School of Architecture and Planning,
in partial fulfillment of the requirements for the degree of
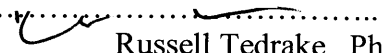
Doctor of Philosophy

at the

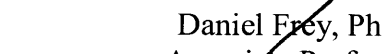MASSACHUSETTS INSTITUTE OF TECHNOLOGY

June 2012

© Massachusetts Institute of Technology 2012

Doctoral Committee

Committee Member: ....

Russell Tedrake, Ph.D.
Associate Professor
Department of Electrical Engineering and Computer Science

Committee Member: ....

Daniel Frey, Ph.D.
Associate Professor
Department of Mechanical Engineering

Acknowledgments

Ad Jesum per Mariam

The work in this thesis was possible thanks to the efforts and contributions of many individuals who deserve my gratitude and recognition. I would like to thank the following individuals, in particular:

My advisor, Prof. Hugh Herr, for all his support and guidance throughout my time at MIT.

The members of the Biomechatronics Group, for their significant contributions to this project over the past years. Particularly, I would like to express my gratitude to Jeff Weber, Grant Elliott, Michael Eilenberg, Bob Emerson, Ken Endo, Jared Markowitz, and Luke Mooney for their invaluable work in the electromechanical designs of the knee prostheses prototypes, and their continual assistance throughout the clinical tests, data analysis, and simulation processes.

Bruce Deffenbaugh, for always being there to provide a word of wisdom and direction.

Prof. Daniel Frey and Prof. Russell Tedrake, for their time and guidance throughout my doctoral research.

My labmates and UROPS Andy Marecki, Jacky Lau, Javier Sanchez, Caitlin Reyda, Luis Carbajal, Claude Lagoda, Andrew Bishara, and Marc Louis for their collaborations in the various phases of the project.

Linda Peterson, Felice Gardner, Tesha Myers and Sarah Hunter, for providing all the necessary resources that enabled my great experience at the Lab.

I would like to thank my family, my parents and sisters for their love and encouragement, and especially my wife Elizabeth for her love and unconditional support throughout the course of the Ph.D.

Contents

List of Figures

List of Tables

Chapter 1

Introduction

Currently available commercial technologies for lower limb amputees are still far from providing fully functional replacements of biological legs. Even with the most advanced prosthetic systems available on the market, above knee amputees still exhibit debilitating clinical problems associated with the lack of adequate mobility, such as gait asymmetry, instability, decreased walking speeds and higher energy requirements. In order to solve these problems, the field of biomechatronics has initiated the development of robotic limbs that can emulate healthy leg behavior. This task poses many challenges for researchers as they investigate novel electromechanical designs and control strategies that can adequately integrate with the patient's body and adapt to the patient's mobility needs.

A significant limitation of conventional technologies in leg prostheses is their inability to provide net positive power output at the joints. This limitation translates into the inability of the prosthesis to restore normal leg functionality and, consequently, in the amputee suffering from clinical problems associated with the lack of mobility and locomotion fatigue. Furthermore, recent development of active powered prostheses has given rise to the pursuit of control strategies that can adequately guide a biological behavior while allowing a more integrated and intuitive human-machine interface.

The biomechanics of normal walking provide a basis for the design and development of new actuated artificial limbs. These prosthetic systems ideally need to fulfill a diverse set of requirements in order to mimic the biological behavior of normal and healthy extremities. In general, some of the main features that should be considered for the design of these prosthetic devices include the capacity to vary stiffness and damping characteristics as well as to provide non-conservative motive power. In addition, these systems must not exceed the weight and dimensional form factor of a comparable intact extremity segment of a healthy/unaffected

person. Moreover, these devices must be adaptive, such that they can change their functional behavior given particular environment disturbances and individual amputees' locomotive needs.

In this thesis, I present the design and implementation of a novel biomimetic active knee prosthesis for transfemoral amputees that is capable of mimicking the behavior of the intact human knee biomechanics. The biologically inspired approach to the design and control of the prosthesis seeks to improve amputees' metabolic requirements, gait symmetry and walking. With this thesis I aim to advance the field of biomechatronics and human-machine integration, contributing to the development of assistive technologies that benefit from the development of biologically inspired models.

The key design architecture and mechanical components of the active knee were established from biomechanical descriptions of the human knee during level ground walking. The knee design is capable of interfacing with conventional prescribed ankle-foot prostheses commercially available. The resulting active knee and ankle biomimetic leg is capable of replicating human-like knee joint mechanics. The active knee presented in this thesis has two main features that contribute to its energetic efficiency: first, it leverages the natural motion dynamics of the leg; second, it uses tendon-like elastic structures to store and release energy, thereby minimizing the power demands on the device actuators.

In order to evaluate the performance and clinical impact of the proposed active leg prosthesis, a series of clinical experiments were conducted with four above-knee, unilateral amputees. This work has been approved by MIT's Committee on the Use of Humans as Experimental Subjects (COUHES). The experiments consisted of three sessions. An initial session qualitatively determined the degree to which the active prosthesis can improve amputee gait. Secondly, an energetic assessment evaluated the impact of the active knee prosthesis on the amputees' metabolic cost of walking and compared the metabolic demand of the prosthesis to that of their prescribed prosthetic technologies. Finally, a biomechanics assessment evaluated joint and motion biomechanics while the amputee walked at self-selected walking speed.

My dissertation work seeks to improve the understanding of the principles of human locomotion and their application in the development of advanced bionic limbs. Both objectives are aimed to improve the lives of the people with physical disabilities.

Clinical trials for this work were registered under name: Active Knee Prosthesis Study for Improvement of Locomotion for Above Knee Amputees. National Clinical Trials Registration ID: NCT00771589 (in clinicaltrials.gov).

Chapter 2

Background

In the United States, there are more than 1.7 people living with limb loss (National Limb Loss Information Center 2008). The total number of persons with an amputation and using a prosthesis is expected to reach 2.4 million by the year 2020 (Ziegler-Graham 2008). In the U.S. alone, above knee amputees exceed 300,000 (NCHS99). Every year more than 30,000 transfemoral amputations are conducted in the U.S. (Feinglass, et al. 1999). As a consequence of lower limb loss, patients present several clinical problems, all associated with lack of mobility and higher energetic demands. Even though currently available prosthetic technology provides certain advantages to amputees, it is still limited, as it is incapable of fully restoring intact leg functionality.

For lower limb amputees, one of the major problems associated with reduced mobility is walking fatigue and pain (Postema, et al. 1997). Although the pain felt at the residual limb is due to the behavior of the entire prosthetic system (i.e. from the liner and socket interface to the pylon and the rest of the prosthetic components), it is particularly associated with the coupling between the residual limb and the prosthetic leg. The imperfect coupling allows relative motion between the socket and the femur stump, caused by the compression of the soft tissue. This motion is uncomfortable for the amputee and causes a lack of confidence in applying large forces to the prosthetic leg. In addition, the relatively short moment arm between the hip joint and the socket reduces the force that the hip muscles can apply to the artificial limb (Whittle 1991). Recent advances in socket technology have reduced pain in patients by focusing on cushioning, a primary contributor to comfort. Such technologies cover a large gamut of products, from gel liners and vacuum-assisted sockets to modern interfaces that rely on residual limb laser scanning and computer aided manufacturing. Two particular technologies that have proved to be successful in pain reduction have been shock absorbing pylons and dynamic elastic response (DER) prosthetic feet (Perry 1992). The damping and compliance features they provide have made them popular in most of the commercially available prosthetic systems. Despite their

success in preference among amputees, abnormal gait patterns associated with walking fatigue are still prevalent.

Walking fatigue is synonymous with higher metabolic expenditure and is a common affliction of lower limb amputees. Walking fatigue in lower limb amputees is considerably higher than their matched able body counterparts at comparable speeds. Measures of metabolic expenditures during walking are commonly obtained by analyzing oxygen level consumptions. For unilateral below the knee amputees, the rate of oxygen consumption is 20-30% higher than that of intact subjects (Herbert, et al. 1994) (Molen 1973), and for above knee amputees there is an additional 25% increment (James 1973) (Waters and Mulroy 1999). Conventional prostheses, despite their damping and compliance features, have not provided a metabolic advantage for amputees (Lehmann, et al. 1993) (Torburn, et al. 1990) (Colborne92) (Huang, Chou and Su 2000) (Thomas, et al. 2000). In addition to higher metabolic consumptions, lower limb amputees show a reduction in their self-selected speed, and in consequence, they present overall diminished endurance.

For above knee amputees, a particular cause of pathological gait is the lack of accurate control of the knee joint during the swing phase. During this phase, the knee cannot be totally free, because it would then extend too rapidly with a sudden stop hitting the boundary in hyperextension. In contrast, the knee joint cannot be so rigid that it does not permit flexion or extension; this would result in an increase of the amount of energy required by the hip muscles to move the prosthesis as a single piece. To prevent these extreme cases, several prosthetic knees have been developed that include friction mechanisms and hydraulic/pneumatic systems, with some of the most advanced systems having electronic control technologies. Some have been designed as variable damping devices that change their behavior depending on the joint angle, speed and direction of motion. These mechanisms have partially solved some of the problems associated with abnormal gait patterns in amputees (Whittle 1991).

A major cause of abnormal gait for transfemoral amputees is the need to walk with the knee in full extension during the single stance support phase, since the amputees cannot provide opposition to an external flexion torque around the knee axis. To prevent this, passive artificial

knees with higher stiffness are generally employed. However, the inconvenience with higher stiffness in the knee joint during the stance phase is that the location of the center of gravity is dramatically affected, increasing the energy needed to walk. Although amputees adapt to this circumstance, this type of walking is energetically demanding for all of patients (Whittle 1991).
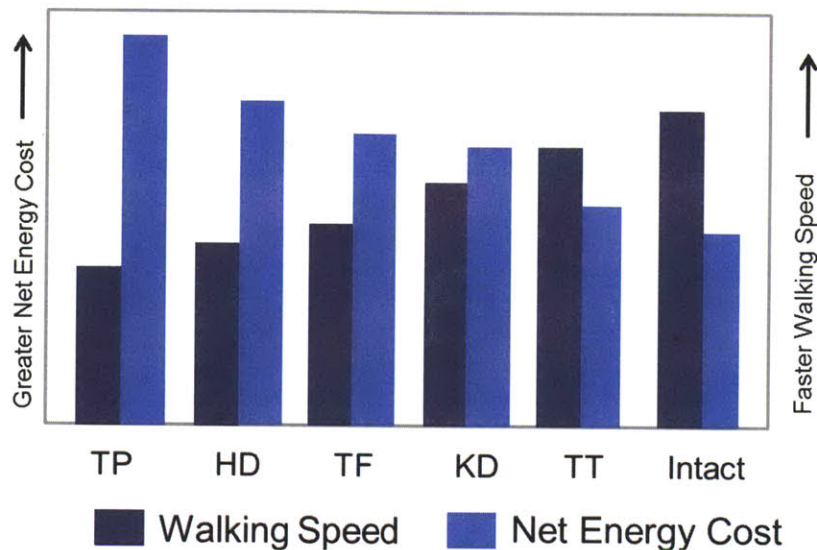
Figure 2.1 . Amputee walking: relative pace and energy consumption((Rose and Gamble 2006) from modified data in (Waters and Mulroy 1999)). Representation of two important trends that compare the relative pace and energy consumption for amputees walking with a lower limb prosthesis. The higher the level of the amputation the slower the self-selected walking speeds becomes in addition to larger net energy required to walk a given distance. TP= tanspelvic amputation; HD= hip disarticulation amputation; TF = transfemoral amputation; KD= knee disarticulation amputation; TT= transtibial amputation; Intact= non-amputee.

For below the knee amputees, the inability to articulate their ankle joint generates an abnormal gait, including gait asymmetries, lower self-selected speeds and higher energy requirements (WinterSienko88) (Molen 1973) (Colborne92). The human ankle joint is essential to walking, as it provides a significant amount of net positive work over the stance period of walking, especially at moderate to fast walking speeds (Winter 1983) (Palmer 2002) (Gates 2004). Since the below the knee amputee cannot actively plantarflex at the end of the stance phase of walking, no power is generated in the push off. The amputee must therefore lift the leg sooner to clear the ground, since the effective length of the leg is reduced compared to a normal limb. There are some commercial prostheses that have a spring-like behavior that help store

some energy during hill strike and stance phase and then release it at toe-off. Although these prostheses have a certain spring-like give which helps them function as initial and terminal rockers, they cannot provide net positive work; as a result, they are not functional enough to replicate a normal ankle's flexibility and actuation (Whittle 1991).

2.1 State of the Art in Lower Extremity Prostheses

Modern transfemoral prostheses can be classified into three major groups: passive, variable-damping, and powered. Passive prosthetic devices do not require a power supply for their operation, and are generally less adaptive to environmental disturbances than variable-damping or powered prostheses.

Variable-damping knees have been some of the most significant advances in active prostheses technology. These knees require a power source to modulate damping levels and adapt to different modes of gait, whereas powered prosthetic knees are capable of performing non-conservative positive work. Variable-damping knees offer several advantages over mechanically passive designs, including enhanced knee stability and adaptation to different ambulatory speeds (Flowers 1972) (Stein, Rolf, James, & Tepavic, 1990) (Kitayama, Nakagawa and Amemori 1992) (Herr and Wilkenfeld 2003) (Johansson, et al. 2005)(Zahedi 1993) . Examples of commercially available variable-damping knees include the Blatchford Endolite Intelligent Prosthesis, the Otto Bock C-leg, and the Össur Rheo.

From these examples, two of the most advanced devices, and the most relevant to the current investigation, are the Otto Bock's C-leg and Genium models. These knees use a microcomputer to adjust the damping characteristics of their hydraulic joint in order to adapt to patients' walking speed and to detect and prevent stumbling, allowing safer ramp and stair descent. A second example of a microcontroller based knee is the Össur's Rheo Knee, developed originally at MIT. This knee prosthesis actively controls a magnetorheological-based fluid that varies damping ratios to allow speed and terrain adaptation.

Although variable-damping knees offer some advantages over purely passive knee mechanisms, they are nonetheless incapable of producing positive mechanical power and therefore cannot replicate the positive work phases of the human knee joint for such activities as sit-to-stand maneuvers, level-ground walking, and stair/slope ascent ambulation. Not surprisingly, transfemoral amputees experience clinical problems when using variable-damping knee technology. For example, amputees have asymmetric gait patterns, slower gait speeds, and elevated metabolic energy requirements compared to non-amputees (Johansson, et al. 2005).

a)　　　　　　　　b)　　　　　　　　c)
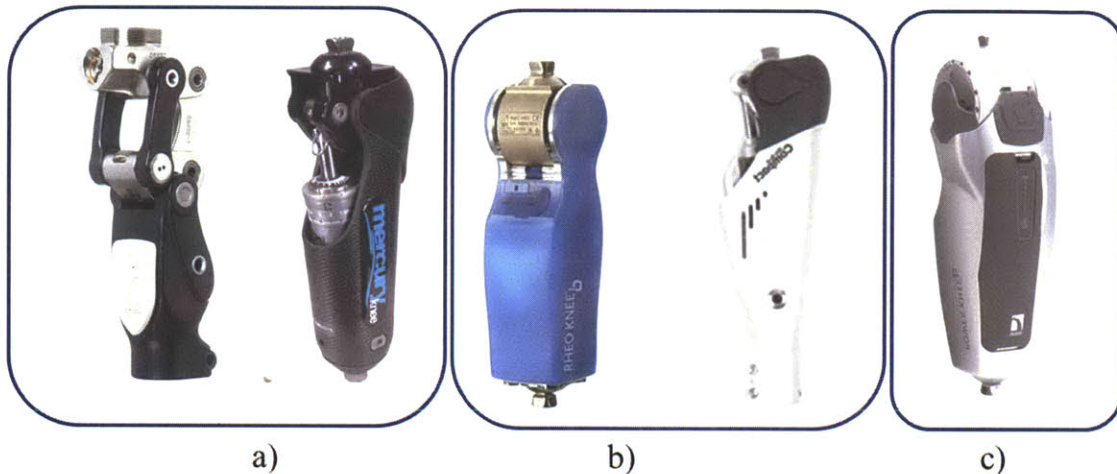
Figure 2.2. Examples of commercially available knee prosthesis. According to their classification from left to right: a) Passive: Ossur® Total Knee and Endolite® Mercury; b) Variable-damping: Ossur® Rheo knee and Otto-Bock® C-leg ; c) Powered: Ossur® Power Knee.

A challenging design problem has been developing a commercially-viable powered prosthesis that is human-like in its weight, size and strength while still being energetically economical and noise-free. Current approaches to the design of powered prostheses have focused mainly on the use of single motor-transmission systems directly coupled to the knee joint (Kapti and Yucenur 2006) (Fite, Mitchell and Goldfarb 2007). (www.ossur.com) Such direct-drive designs, however, require high electrical power consumption to emulate fully the mechanical behavior of the human knee joint even during level-ground ambulation. Perhaps one reason for this lack of energetic economy is that such designs do not adequately leverage the passive dynamics of the leg, and the elastic energy storage and return of tendon-like structures, in a manner comparable to highly economical walking machine designs (McGeer, 1990) (Wisse

2004) (Endo, Paluska and Herr 2006) or simpler mechanical knee designs with extension assist compliant elements (Radcliffe 1977).

The development of powered foot-ankle prostheses for transtibial amputees is less far advanced. Ossur has introduced the first commercially available "powered" ankle prosthesis named "Propio Foot," which does not provide net power during the gait. Instead, it can actively adjust the dorsiflexion angle to avoid stumbling during walking and to allow a better sitting posture (Koniuk 2001). Au and Herr at MIT introduced the world's first powered foot-ankle system capable of providing an improved metabolic economy to below-knee amputees. This prosthesis is capable of both varying joint impedance during stance and providing sufficient instantaneous power output and torque during push-off in order to propel the amputee during level-ground walking (Au, Martinez-Villalpando and Herr, Powered Ankle-Foot Prosthesis for the Improvement of Amputee Ambulation 2007) (S. Au 2007) (Au and Herr 2008). Hitt et al have built an active robotic ankle prosthesis with anterior-posterior and medio-lateral actuation (Hitt, et al. 2006). Collins and Kuo introduced controlled energy storage and release prosthesis (CESR) for below knee amputees, capable of efficiently storing energy during stance and adequately timing its release in order to help amputees improve their gait (Collins and Kuo 2010). Transfemoral prostheses that include both powered knee and ankle system are limited. Sup et al have built a tethered, electrically powered knee and ankle prototype (Sup, Bohara and Goldfarb 2008) and more recently presented an electrically powered self-contained active and ankle prosthesis (Sup, Varol, et al. 2009).

Chapter 3

Knee Biomechanics

In this chapter, the human knee biomechanics for level ground walking are reviewed. Based on the biomechanical functional description of the intact knee joint, a mono-articular variable-impedance prosthetic knee model is presented. This model is then used to motivate the electromechanical design architecture of the active knee prosthesis.

3.1 Intact human knee biomechanics in level ground walking

In order to inform the design of the active knee prosthesis, it is important to study the biomechanics of the intact human knee joint. Human walking is a periodic behavior, and its representative period is called a gait cycle (GC). For level-ground walking, the gait cycle is commonly defined as the period between successive heel-strikes of the same extremity. The GC has two main phases: stance and swing. Stance phase, defined as the period in which the foot of the observed extremity is on the ground, takes approximately the first 60% of GC, and the swing phase (while the foot is off the ground) takes the rest. Both of these phases can be divided into subphases. In the following section, I describe the main subphases in the GC, focusig on the biomechanical description of the knee joint. For the purposes of this thesis, the analysis and description of the knee behavior consider only the sagittal plane.

Five distinct stages or gait phases have been used to describe knee biomechanics in level-ground walking: (see figure 3-1):

1. *Stance Flexion*. Beginning at *heel strike (HS)*, the knee begins to flex slightly (~15 degrees). This early stance phase allows for shock absorption after initial contact with the ground.

2. ***Stance Extension.*** After maximum stance flexion (MSF) is reached, the knee joint begins to extend (15% gait cycle), until maximum stance extension (MSE) is reached (42% gait cycle).

3. ***Pre-Swing.*** Occurring in late stance (from 42% to 62% gait cycle), the knee of the supporting leg begins its rapid flexion period in preparation for the *Swing* phase. The knee begins to flex in preparation for toe-off.

4. ***Swing Flexion.*** As the hip is flexed, the leg leaves the ground and the knee continues to flex. At toe-off, the *Swing Flexion* phase of gait begins. Through this period (from 62% to 73% gait cycle), knee power is generally negative as the knee's torque reduces knee rotational velocity.

5. ***Swing Extension.*** After reaching a maximum flexion angle (~60 degrees) during *Swing*, the knee changes direction and begins to extend. During *Swing Extension* (from 73% to 100% gait cycle), knee power is generally negative to decelerate the swinging leg in preparation for the next stance period. After the knee has reached full extension, the foot, once again, is placed on the ground, and the next walking cycle begins.

From the biomechanical description of the knee in each of this subphases, a general model description of the knee behavior is extracted. This modeled behavior can be divided again in the two main phases of gait, stance and swing.

During stance flexion-extension and pre-swing, the knee can be modeled with spring-like elements (observe the torque vs. angle slope in figure 3-1B). In stance flexion, a linear elastic element stores energy in preparation for the *Stance Extension*. In stance extension, the knee continues to behave as a spring with similar stiffness[1] to that of *Stance Flexion*. Furthermore, in pre-swing, as the knee flexes in preparation for toe-off, the spring-like behavior of the knee is maintained but with relatively lower stiffness as compared to *Stance Flexion and Extension*.

After toe-off and throughout swing, knee power is predominantly negative. During swing flexion the knee torque reduces knee rotational velocity before reaching a maximum knee

---

[1] Here stiffness is not actual joint stiffness but rather a quasi-static stiffness defined as the slope of the torque vs. angle curve.

flexion angle. After changing direction, and as the lower leg extends, knee power is mainly negative, decelerating the swinging leg and reducing terminal impact in preparation for the next heel-strike that starts the new gait cycle. Knee behavior during swing flexion and extension phases exhibits a predominant negative joint power, thus allowing this behavior to be captured primarily with a variable damper.

3.2 Quasi-passive prosthetic knee model

Given the knee biomechanics descriptions and model insights from the last section, we anticipate that a variable-impedance knee prosthesis, capable of varying both damping and stiffness, can produce human-like knee mechanics during steady-state level-ground walking. As a first evaluation of this hypothesis, and to motivate the design of the prosthesis, a prosthetic knee model is proposed (shown in figure 3.2), comprising two antagonistic series-elastic clutches (to model the stance phase knee mechanics) and one variable-damping element (to model the swing phase mechanics). In the model, a series spring can be engaged by activating its respective clutch, or disengaged by opening that clutch. A constraint of the model is that each clutch can be engaged only once during each gait cycle. Additionally, once a clutch has been engaged, it only can be disengaged when the series spring has released all its energy and the force on the clutch is zero.
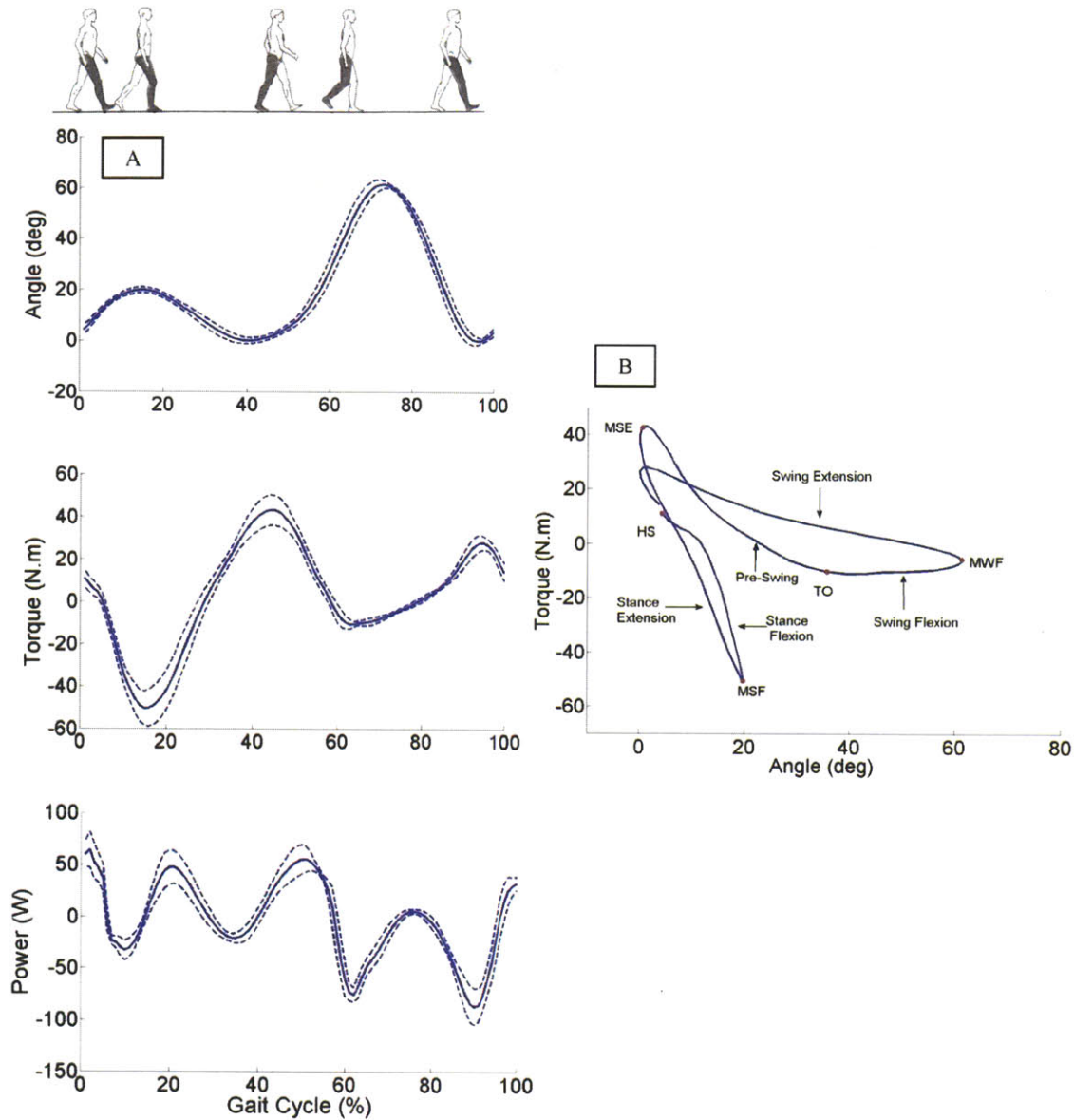
Figure 3.1- Representative knee biomechanics in level-ground walking. In (A), the knee angle, torque, and power curves of a mid-size average male subject (mass = 81.9 kg) are plotted against percent gait cycle during level ground walking at a self selected speed (1.31 m/sec). Plotted are mean (solid line; N=10 gait trials) about one standard deviation (dashed lines). In (B), knee torque is plotted vs. knee angular position showing the five phases of gait. Key gait events separating the five phases are: HS, heel strike; MSF, maximum stance flexion; MSE, maximum stance extension; TO, toe off; and MWF, maximum swing flexion.

We varied series-elastic clutch model parameters: two spring constants (k_E, k_F) corresponding to the extension[2] and flexion spring stiffness, and the relative knee extension and flexion equilibrium angles (θ_E and θ_F) at which the extension and flexion springs engage during stance.

The knee model was fitted to biomechanical data using an optimization scheme that minimized the sum over time of the squared difference between the model's knee joint torque and biological knee values. More specifically, the cost function used for the optimization was

$$E_{\cos t}(k_F, k_E, \theta_E, \theta_F) = \sum_{i=1}^{100} \left(\frac{\tau^i_{bio} - \tau^i_{sim}}{\tau^{max}_{bio}} \right)^2 \qquad (3.1)$$

where τ^i_{bio} and τ^i_{sim} are the angular torques applied about the knee joint at the ith percentage of gait cycle from the biological torque data and the knee model, respectively, and τ^{max}_{bio} is the maximum biological torque at the joint during the gait cycle. Cost function (1) was minimized with the constraint that the extensor spring always engages at heel strike ($\theta_E = 0$). We applied this constraint to limit knee buckling at heel strike as a safety measure for the amputee. The determination of the desired global minimum for cost function (1) was implemented by first using a standard genetic algorithm (gatoolbox MATLAB®) to find the region containing the global minimum, followed by an unconstrained gradient optimizer (*fminunc* function application in MATLAB®) to determine the exact value of that global minimum. After optimizing cost function by varying the parameters of the series-elastic clutch elements, the model's variable damper was used to achieve perfect agreement between the prosthetic knee model and biological torque values in regions where the series-elastic components were not able to absorb sufficient negative mechanical power.

The biological knee torque values were obtained from an inverse dynamics calculation using kinetic and kinematic data from ten walking trials of a healthy subject (81.9 kg, 1.87m in height walking at 1.31 m/s). The subject was chosen as a representative mid-size average male that fits the 50% percentile description for US adults (Tilley, A R; Henry Dreyfuss Associates

---

[2] By convention, the extensor spring tends to extend the knee joint when engaged, whereas the flexor spring tends to cause the knee to flex.

2002). A detailed description of how these kinetic and kinematic data were collected and analyzed is presented in the next section, *Intact-subject walking: data collection and analysis*.
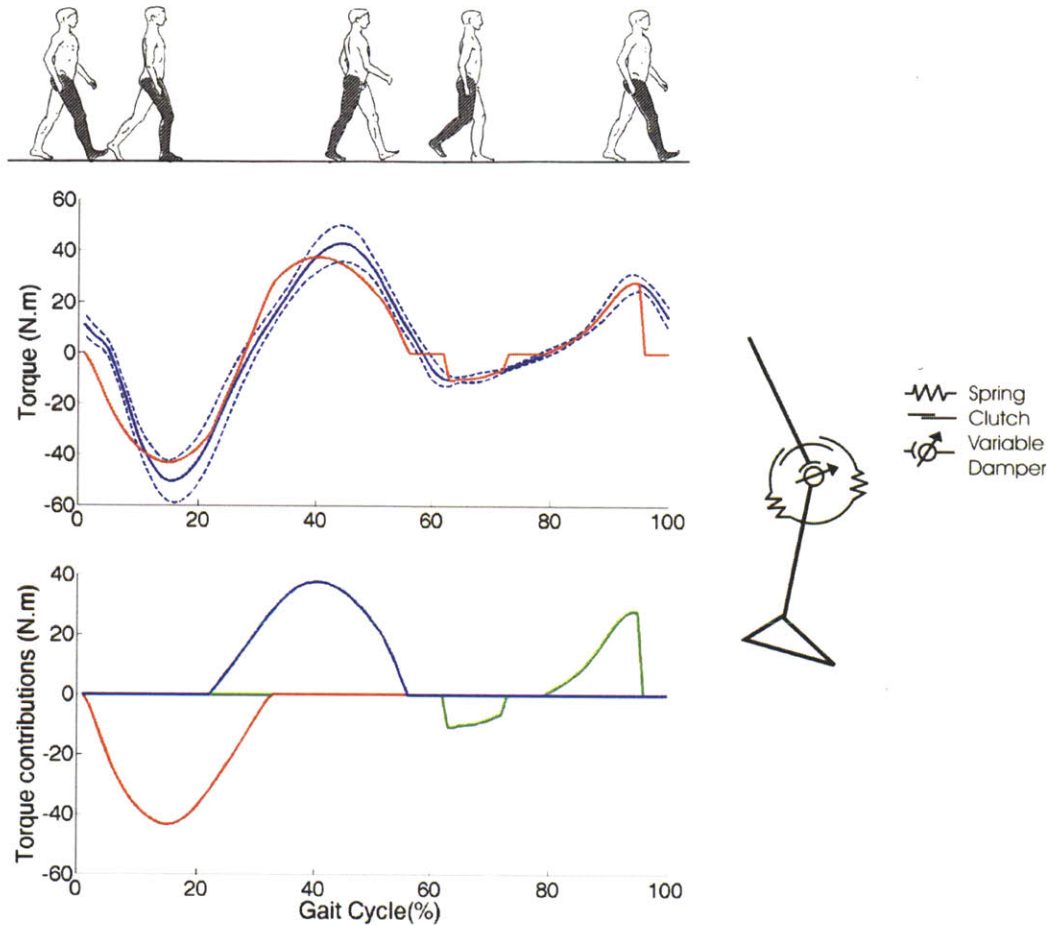
Figure 3.2- Variable-impedance prosthetic knee model. The model, shown on the right, comprises two mono-articular series-elastic clutches and a variable-damping element. In the upper plot, optimized net torque output of the knee model (red line) is compared to the torque profile of an intact human knee joint (mean is solid blue line; one standard deviation is dashed blue line; N=10 gait trials). Biological data, adopted from figure 3.1, are from a study participant (mass = 81.9kg) with intact limbs walking at a self-selected speed (walking speed = 1.31 m/sec). Shown in the lower plot are the torque contributions from the extension (red line) and flexion (blue line) springs of the series-elastic clutch elements, as well as the variable damper (green line). The optimizer gave an extension spring stiffness equal to $k_E = 160$ N.m/rad, a flexion spring stiffness equal to 137 N.m/rad, and a knee engagement angle for the flexion spring equal to 0.27 radians (15.46 degrees). The extension spring was constrained to engage at the instant of heel strike.

24

Figure 3.2 shows the model optimization results plotted against the biological torque data from figure 3.1. The model's torque output agrees well with experimental values. As constrained by the optimization procedure, the extension spring engages at heel strike, storing energy during early stance knee flexion. As the knee begins to extend, the flexion spring is engaged, storing energy as the extension spring releases its energy. During the swing phase, the model's variable damper exactly matches the biological torque values in regions of negative power. At mid and terminal swing phase, the power is positive in the biological data, and thus, the damper outputs zero torque in these gait regions.

3.3 Intact-subject walking data collection and analysis

Intact-subject kinetic and kinematic walking data were collected at the Gait Laboratory of Spaulding Rehabilitation Hospital, Harvard Medical School, in a study approved by the Spaulding committee on the Use of Humans as Experimental Participants. One healthy male adult participant volunteered for the study. The participant was asked to walk at a self-selected speed across a 10m walkway in the Motion Analysis Laboratory, for ten consecutive trials. He was timed between two fixed points to ensure that the same walking speed was used between experimental trials. Walking speeds within a ±5% interval from the self-selected speed were accepted. The data collection procedures were based on standard techniques (Winter D. , 1990)(Kadaba, Ramakrishnan and Wootten 1990). An infrared camera system (eight cameras, VICON 512 motion analysis system, Oxford Metrics, Oxford, UK) was used to measure the three-dimensional locations of reflective markers at 120 frames/s. A total of 33 markers were placed on various parts of a participant's body using the standard Plug-in Gait model: 16 lower-body markers, five trunk markers, eight upper-limb markers and four head markers following. The markers were attached to the following bony landmarks: bilateral anterior superior iliac spines, posterior superior iliac spines, lateral femoral condyles, lateral malleoli, forefeet and heels. Additional markers were rigidly attached over the mid-femur and mid-shaft of the tibia. The kinematics of the upper body were also collected with markers placed on the following locations: sternum, clavicle, C7 vertebra, T10 vertebra, head, and bilaterally on the shoulder,

elbow and wrist. The VICON 512 system was able to detect marker position with a precision of ~1mm.

During walking trials, ground reaction forces were measured synchronously with the kinematic data at a sampling rate of 1080Hz using two staggered force platforms (Advanced Mechanical Technology Inc. -AMTI, Watertown, MA, USA) embedded in the walkway. The platforms measured ground reaction force and center of pressure location at a precision of ~0.1N and ~2mm, respectively. Prior to modeling and analysis, all marker position data were low pass filtered using a 4th order digital Butterworth filter at a cutoff frequency of 8Hz. Filter frequency was based on the maximum frequency obtained from a residual analysis of all marker position data, and processed as one whole gait cycle with 100 discrete data points from the heel strike to the next heel strike of the same leg. Joint torques and powers were then calculated using a standard inverse dynamics model (Vicon Bodybuilder; Oxford Metrics, UK).

Chapter 4

Mechanical Design

Developing a powered prosthesis that is human-like in weight, size and functionality, while still being energetically-efficient and noise-free, is indeed a challenging task. Current approaches to the design of powered prostheses have focused mainly on the use of single motor-transmission systems directly coupled to the knee joint (Kapti and Yucenur 2006) (Fite, Mitchell and Goldfarb 2007) (www.ossur.com). Such direct-drive designs, however, require a high electrical power consumption to emulate fully the mechanical behavior of the human knee joint even during level-ground ambulation. One reason for this lack of energetic economy, perhaps, is that such designs do not adequately leverage the passive dynamics of the leg and the elastic energy storage and return of tendon-like structures in a manner comparable to highly economical walking machine designs or simpler mechanical knee designs with extension assist compliant elements (Radcliffe 1977).

From the biomechanical knee descriptions and gait biomechanics, the main design goals for the prosthesis that should be considered are categorized as follows.

4.1 Main Design Specifications

Size and weight. The overall design of the knee prosthesis considers the dimensions of average mid-size U.S. male subject that fits the 50% percentile anthropometric dimensions and weight distribution ((Tilley, A R; Henry Dreyffus Associates, 2002) (Winter, Biomechanics of Motion of Human Movement 2005)). For this average subject, intact lower leg length measured from the femoral condyles to medial malleolus corresponds to an average of 42.2 cm. Taking into account socket for the residual limb, as well as standard distal and proximal prosthetic knee connectors and adaptors to the socket and foot-ankle prosthesis the design goal criteria for knee

prosthesis' length is a maximum of 35 cm.   The biological segment of lower extremity based on the same landmarks mentioned earlier is on average 4.65% of body weight according to body segment estimates obtained from (Winter, Biomechanics of Motion of Human Movement 2005) (Durkin and Dowling 2006). The prosthesis, considering an average intact male subject, should not exceed a total mass of 3.6 kg. Furthermore, the electromechanical structure of the knee should remain within the biological volumetric envelope of the biological counterpart for aesthetic symmetry purposes.

Flexion and extension range. In level-ground walking from slow to fast speeds, the knee angle does not surpass $65°$ of flexion (during maximum swing flexion) (Winter D. A., 1983). However, the design of the knee should consider other activities with higher flexion angles such as sitting/standing maneuvers and stair ascent/descent where the maximum observed knee flexion angle is can reach up to $105°$ (Riener, Rabuffetti and Frigo 2002). The knee prosthesis then should accommodate such flexion angle range.

Joint output torque. For an average able body intact subject walking from slow to fast speeds on level-ground, requires an average maximum knee torque of 60 N.m (Winter D. A., 1983). However for stair ascent and descent, larger torques are required. A maximum of approximately 120 N.m for a mid-size subject in stair descent is measured (Riener, Rabuffetti and Frigo 2002) . We used this value as the target output torque specification for the active knee design. Moreover, the motion bandwidth of the knee in level ground walking should have at least a bandwidth of 2 Hz. This value is an average observed in intact humans at moderate self-selected walking speeds (Winter D. A., 1983).

4.2 Mechanical Design Architecture

Motivated by the prosthetic knee model described in Chapter 3, a novel active knee prosthesis design architecture is proposed. This novel design is a result of earlier work developed by the author at the Biomechatronics Group (Martinez-Villalpando and Herr 2009; Martinez-Villalpando et al. 2008 (2) and 2011).

This active knee prosthesis is comprised of two actuators arranged in parallel with agonist-antagonist architecture. Each of the two actuators provides an independent extension and a flexion motion respectively. The extension actuator is bidirectional, and the flexion actuator is unidirectional. Each actuator of the knee prosthesis consists of a motor and a series-elastic element, connected via a transmission. The extension and flexion actuators can be used independently to control the knee angle. Because of its architecture, this knee architecture can be controlled in order to behave with a clutchable series elasticity during the stance phase, and as a variable-damper during the swing phase. This design architecture is hypothesized to serve as a basis of a knee prosthesis that is energy efficient for level-ground walking.
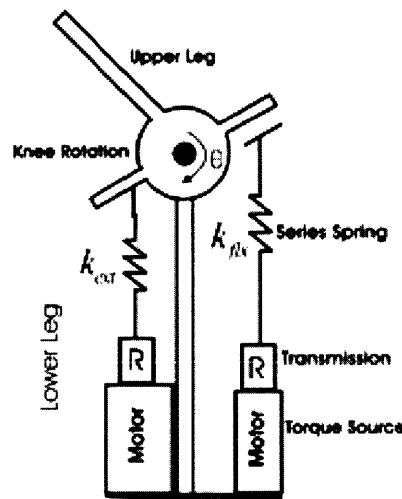
Figure 4.1- Prosthesis Design Architecture. A simplified mechanical schematic of the agonist-antagonist knee.

It is important to note that since the knee design is fully motorized, knee joint torque can be directly controlled for more energetically expensive tasks, such as ascending stairs or inclined terrains, as well as standing from a seated posture. Hence, the knee architecture is designed to accommodate non-conservative, high mechanical power movements, while still providing for a highly economical level-ground walking mode.

4.3 Mechanical Design Description

4.3.1 Series Springs - The flexion and extension springs for the knee prosthesis were selected based on the knee model optimization values performed in chapter 3. These springs

were selected in in order to accommodate a knee design for an average mid-size U.S. male subject (50% percentile). The selected moment arm from each actuator to the output joint is of 2.54 cm (equivalent to 1 in). This moment arm matches the distance from knee joint rotation axis to socket pyramid connector seen in other commercial prosthetic devices. Given the maximum angular displacement the knee joint exhibits during stance while walking at fast speeds (Winter D. A., 1983), (faster walking speeds exhibit greater joint displacements) we estimated the maximum compression of such springs. This allows us to determine their minimum length in order to choose a spring that can maintain an ideal operating range.

According to data presented in (Winter D. A., 1983), the maximum knee flexion in stance during fast walking is ~19° and the maximum knee extension is ~15°. We assume the extension and flexion springs can be engaged through the whole range of those flexion and extension motions respectively. With a 2.54 cm moment arm, the maximum linear displacement of the springs is of 0.84 cm and 0.66cm for the extension and flexion springs respectively. Generally a spring cannot be compressed more than 40% of their free length in normal operation, particularly those that are meant for medium to high duty applications. With this constraint, the minimum desired length for such springs should be of 2.15 cm for the extension spring and 1.65 cm for the flexion springs.

The series springs selected for the extension and flexion actuators are both commercial helical coil compression die springs (linear). The extension actuator has two pre-compressed identical spring in a typical bidirectional series elastic actuator (described in the next section). These springs are Century's spring ® model D-52, medium duty oil-tempered steel spring with nominal free length of 1 in (2.54 cm). The flexion actuator has a single spring element, Lee spring® LHL 1000C 01 heavy duty die spring with nominal free length of 1 in (2.54 cm)

A characterization of those springs was performed using an Instron® machine in order to verify their stiffness values and calibrate sensor readings. A summary of their specifications is shown in table 4.1.
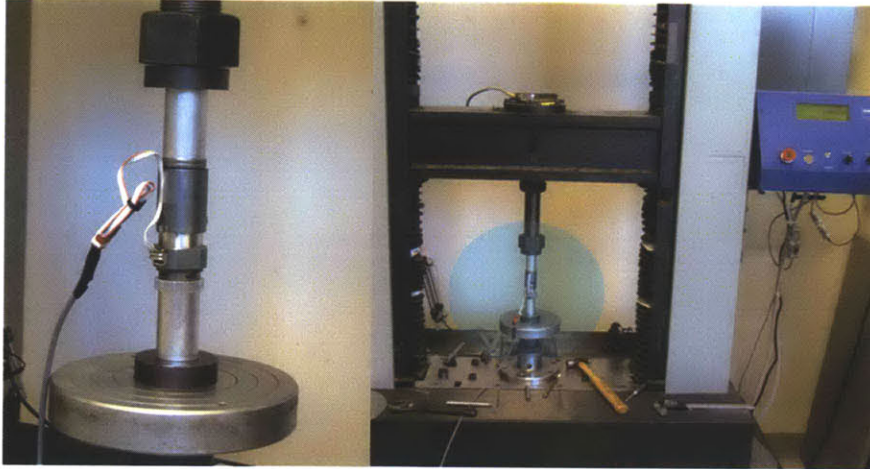
Figure 4.2- Characterization of spring stiffness using Instron® machine

Series Elastic Spring Element	Simulation Stiffness	Manufacturer-Model	Nominal Stiffness	Measured Stiffness
Extension (x2)	248 kN/m (160 Nm/rad)	Century Spring ® D-52	252 kN/m (162 Nm/rad)	258 KN/m 166 Nm/rad
Flexion	212 kN/m (137 Nm/rad)	Lee Spring® LHL 1000C 01	192 kN/m (124 Nm/rad)	224 KN/m (145 Nm/rad)

Table 4.1 . Series elastic components of extension and flexion actuators

4.3.2 Actuator and Transmission - The flexion and extension actuators system should be capable of providing the desired torque-velocity trajectories during level ground walking, ensuring that the motors in the system will not saturate. Thus, the desired knee behavior should remain within the ideal actuator bounds. We characterized the maximum limit performance for both knee actuators during steady state in order to verify their performance and confirm the selection of the motor/transmission system elements.

The extension actuator is bidirectional, and the flexion actuator is unidirectional. The extension actuator and flexion actuator can be used independently to control the knee joint angle at which the series springs can be engaged.

Extension Actuator

The extension actuator, proximal to the knee joint of prosthesis, consists of an extension motor and a set of two pre-compressed series springs, connected via a two stage transmission. The extension transmission consists of a timing pulley set and belt drive system coupled to a precision ball-screw drive.

The extension actuator's electric motor is a brushed 24 V DC motor (Maxon® RE30). In the first stage of the transmission, the extension motor directly drives a timing pulley-belt drive mechanism. This mechanism has a 1:2.66 transmission ratio. In a second stage, the timing pulley-belt drive mechanism actuates the rotation of a ball-screw (Nook ®industries, 10 x 3 mm). When the ball-screw of the extension actuator rotates, there is a linear displacement of the coupled ball-nut support. The ball-nut support is directly attached to the extension series-elastic spring enclosure. The total transmission ratio after the dual stage is of $R = 134.8$.
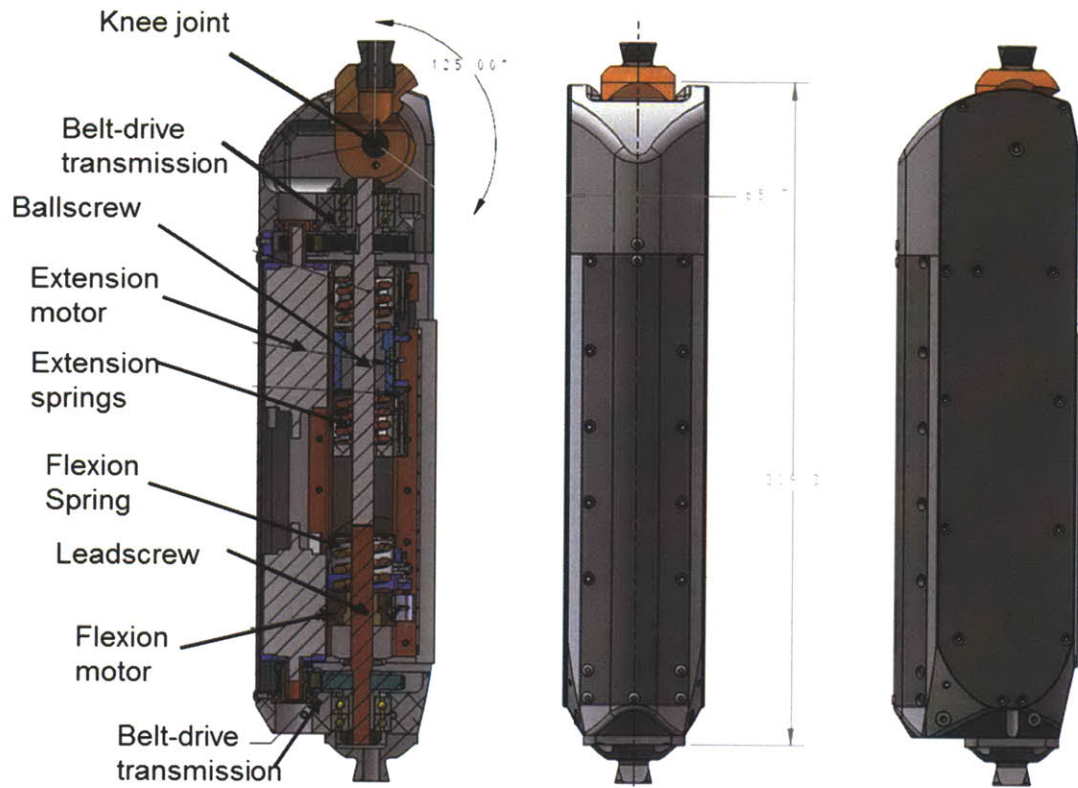
Figure 4.3-Mechanical design of the antagonistic active knee prosthesis

The extension series-elastic spring enclosure securely contains a spring set of the two identical pre-compressed passive mechanical springs. Their stiffness closely matches that of the model's extension actuator. Thus, when there is a linear displacement of the coupled ball-nut support, the extension series elastic enclosure/cage has a linear displacement. The ball-nut support moves along two custom linear steel guide rails. Each of the rails is attached to a corresponding lateral wall housing. The spring cage moves along the guide rails supported by its incorporated roller bearings. The extension actuator is directly coupled to the rotary motion of the knee joint as it is attached to the steel cable drive system.
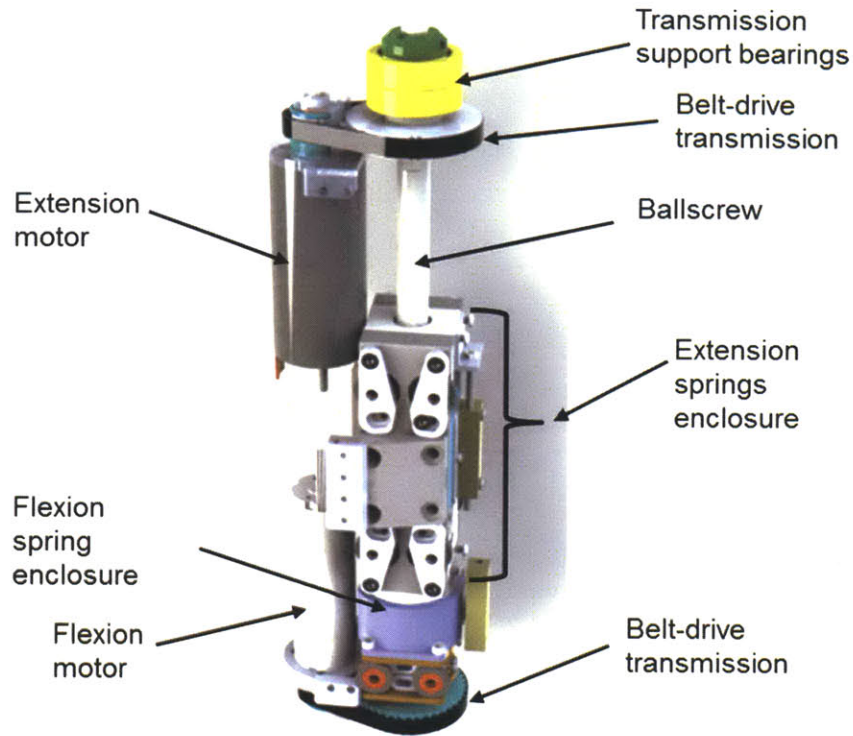
Figure 4.4-Antagonistic motor-transmission assembly
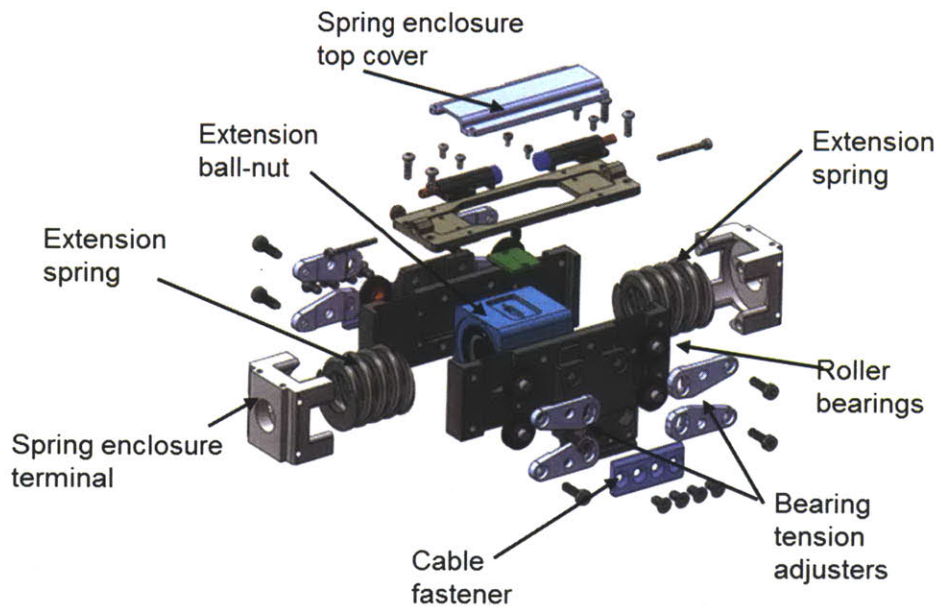
Figure 4.5-Linear carriage/spring enclosure mechanism for series elastic extension actuator.

Flexion Actuator

The unidirectional flexion actuator of the knee prosthesis consists of the flexion motor and a series spring, connected via a transmission. The flexion transmission also has a dual stage. The first stage consists of a timing pulley set and belt drive system coupled to second stage consisting in a lead-screw drive.

The flexion actuator's electric motor is a brushed 24 V DC motor (Maxon® RE30) similar to the extension actuator. The flexion motor directly drives a timing pulley-belt drive mechanism with a 1:2.66 transmission ratio. The pulley-belt drive mechanism actuates the rotation of a lead-screw (Nook® industries, 10 x 3 mm). The rotation of the lead-screw causes a linear displacement of the coupled ball-nut support that directly attaches to the single flexion series spring enclosure or cage. This cage securely contains the flexion spring. The stiffness of this spring is closely matches that of the model discussed in Chapter 3. The ball-nut support moves linearly along two linear steel guide rails supported with low-friction roller bearings incorporated in the ball-nut support. The flexion actuator is not directly coupled to the rotary motion of the knee joint; however, it can flex the knee when in action, back-driving the extension's series elastic spring enclosure.

	Actuator	Motor	Transmission reduction $R = 134.8$	
			Stage 1	Stage 2
Flexion	Unidirectional	Brushed 24 V Maxon® RE30	SDP Belt-Drive [1: 2.66]	Nook® Lead-screw [10 x 3 mm]
Extension	Bidirectional	Brushed 24 V Maxon® RE30	SDP Belt-Drive [1:2.66]	Nook® Ball-screw [10 x 3 mm]

Table 4.2. Active knee prosthesis motor - transmission systems

The knee electromechanical design can accommodate more powerful motors, including brushless DC motors for the extension and flexion actuators (such as Maxon® EC-powermax 30

and 22) in substitution for the DC motors currently used. This modification would require a change in the electronics suite in order to drive such motors. With brushless motor technology, the knee can reduce its overall weight and increase its torque/power capabilities. The author decided to use a DC motor for this design in order to simplify the electronics requirement and evaluate the clinical impact of the prototype. Once this impact is established, the decision to pursue the installation of different motor technology could be evaluated.
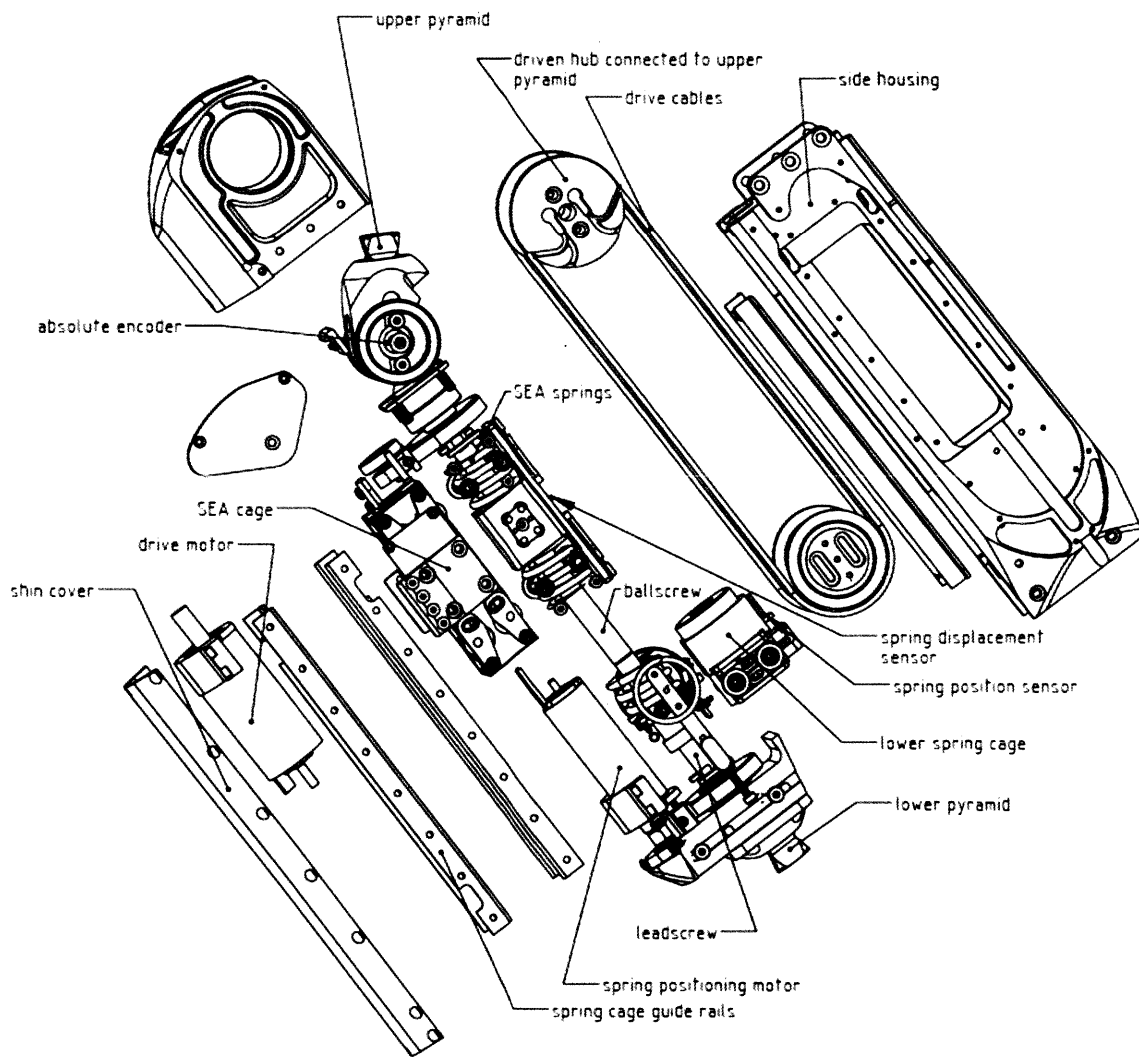
Figure 4.6- Main components of active knee prosthesis (disaggregated view).

The knee joint is rigidly coupled to a set of two steel cable drives connected to the extension's series elastic spring cage. The series elastic cage is supported and guided by two steel precision guide rails. The steel cables allow the coupling of linear displacement from the series

elastic spring enclosure to the rotary motion of the knee joint. The two ends of each of the steel cables are attached to the knee joint's driving hubs. The driving hubs are supported by the knee joint housing. Each cable loops around its corresponding joint pulley located on each side of the knee, distally from the knee joint. Each lateral joint pulley has its axis attached to its corresponding lateral wall. Each cable drive can be independently tensioned with an adjustment to the lateral joint pulley via the tuning of a corresponding cable tensioner.

All actuation mechanisms are fully supported by an aluminum structure that acts as a chassis composed of the lateral knee walls, a distal pyramid adaptor and a proximal pyramid adaptor. This structure provides a support frame that resembles and fits within the lower limb anatomical volumetric envelope. The lower pyramid adaptor of the knee allows for conventional and advanced robotic foot-ankle prosthesis to be attached. The standard prosthetic upper pyramid adaptor (proximal connector) allows the knee prosthesis to be securely attached to a regular transfemoral socket with standard adaptors worn by amputees. The design of the prosthesis facilitates maintenance, having the chassis include detachable lateral and frontal covers that allow easy access to internal actuators and mechanisms.

The fully assembled system is depicted in the following images. This system includes a custom electronic system suite integrated in the posterior section of the knee joint (described in the next chapter).

Figure 4.7-Biomimetic agonist-antagonist active knee prosthesis

Specification	Intact healthy limb	Active knee prosthesis
Length	35cm	30.9 cm
Medio-lateral width	11cm	6.6 cm
Anterior-posterior width	14cm	7.0 cm
Total weight	3.5kg	2.7 Kg
Flexion angle range	0-105°	0-125°
Maximum output torque	120 N.m	130 N.m
Torque bandwidth	2 Hz	12-14 Hz

Table 4.3 Knee size, angular range, and maximum torque values.

Figure 4.8-Active knee prosthesis dimensional fit to a model of an average mid-size male subject.

4.4 Mechanical Analysis

4.4.1 System Model

The antagonistic knee prosthesis can be represented by a linear lumped-parameter model. The model for each of its actuators is based on the series elastic actuator (SEA) representation (Pratt and Williamson 1995). The motor is modeled as a torque source acting on its motor inertia I_{motor} and motor damping b_{motor}. The motor is modeled in series with a spring of rotary stiffness K_s through a transmission of ratio R.

The equivalent motor inertia Me and equivalent damping be described after the transmission drive of ratio R can be approximated as: $M_e \approx I_{motor} R^2$ and $b_e \approx b_{motor} R$, respectively.

The model of the SEA's torque output T_o, provided a requested (input) torque T_{req} can be approximated as a second order system. The effective requested torque T_e that considers the transmission R can be expressed as $T_e = T_{req}R$ where T_{req} can be related to motor requested current i_{req} and the motor torque constant K_t through the relationship $T_e = T_{req}R = i_{req}K_tR$

Thus, for the single SEA the second order model in the s domain is

$$\frac{T_o(s)}{T_e(s)} = \frac{K_s}{M_e s^2 + b_e s + K_s} \qquad (4.1)$$

The model parameters of the second order system are evaluated for each of the actuators and are presented in section 4.4.3.

Each of the actuators in the active knee prosthesis was analyzed following the SEA system model description. In particular, for the knee prosthesis design, each motor in the antagonistic architecture is modeled as a torque source T_{flx} and T_{ext} for the flexion and extension motors, respectively.

- Each motor has a rotary internal inertia $I_{motor} = \{\, I_{flx}\,; I_{ext}\,\}$ and is applying a force to its respective series spring $K_s = \{\, k_{ext},\ k_{flx}\,\}$ through a transmission R, where k_{ext} and k_{flx} represent stiffness terms.

- The damping terms b_{flx} and b_{ext} represent brush and bearing friction acting on the motors.

- The transmission has a ratio R that converts rotary motion of the motor into linear compression of the series spring. The series spring applies a force with a moment arm of r acting on the knee joint .

- Further, T_k and θ are the external knee joint torque and angular displacement, respectively. This model considers the lower leg inertial properties I_k.

- For simplicity, we convert this rotary model into the translational domain. Effective inertial masses $M_{e,flx}$, $M_{e,ext},$ damping $b_{e,flx}$ and $b_{e,ext}$, and linear motor forces $F_{e,flx}$ and $F_{e,ext}$ are considered.
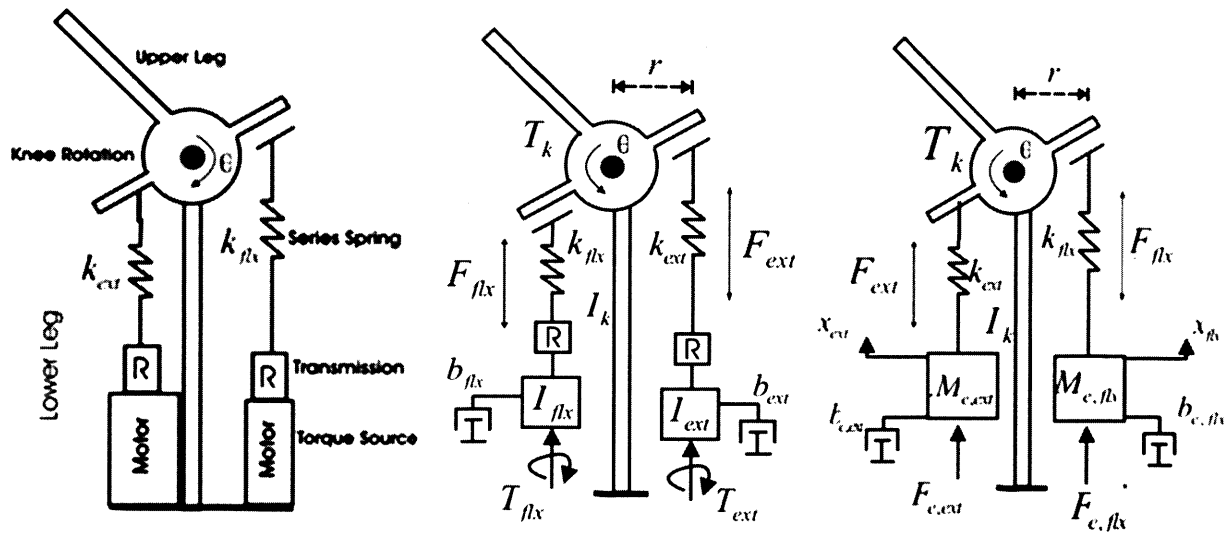
Figure 4.9-Schematics of the agonist-antagonist active knee prosthesis. Representation of the linear prosthesis model in rotary domain followed by the linear model in the translational domain.

41

To simplify the model, we ignore any nonlinearity due to stick-slip friction and backlash as well as any amplifier dynamics. We assume that the transmission ratio is constant and that it does not vary with knee angle. Internal resonances were not considered.

The linear lumped-parameter models that can represent each of the actuators in the knee prosthesis can be described as:

For flexion actuator:

$$M_{e,flx} = I_{flx}R^2 \text{ , } F_{e,flx} = T_{flx}R, \text{ and } b_{e,flx} = b_{flx}R \qquad (4.2)$$

For extension actuator:

$$M_{e,ext} = I_{ext}R^2 \text{ , } F_{e,ext} = T_{ext}R, \text{ and } b_{e,ext} = b_{ext}R \qquad (4.3)$$

The equations of motion then become:

For flexion actuator:

$$M_{e,flx}\ddot{x}_{flx} + b_{e,flx}\dot{x}_{flx} = F_{e,flx} - F_{flx} \qquad (4.4)$$

$$F_{flx} = k_{flx}(x_{flx} - r\theta) \qquad (4.5)$$

For extension actuator:

$$M_{e,ext}\ddot{x}_{ext} + b_{e,ext}\dot{x}_{ext} = F_{e,ext} - F_{ext} \qquad (4.6)$$

$$F_{ext} = k_{ext}(x_{ext} - r\theta) \qquad (4.7)$$

where F_{flx} and F_{ext} are the forces applied by the series springs in the flexion and extension actuators, respectively.

The total external joint torque is then defined as

$$T_k = I_k\ddot{\theta} + rF_{flx} + rF_{ext} \qquad (4.8)$$

4.4.2 Steady State Performance

The actuators of the active knee prosthesis should be capable of producing the desired torque-velocity trajectories exhibited by the biological knee joint during level ground walking. To ensure this capability, the biological behavior should remain within the ideal actuator bounds. In other words, given the selection of transmission, the actuator motors in the system should not saturate while producing such biological trajectories. These trajectories should remain within maximum performance limitations for both of the knee actuators during steady state.

This steady state performance analysis disregarded torque sources other than the selected motor (friction, compliance element, etc). The motor was considered to have direct drive connection to the output joint via the selected transmission (considered to be ideal). The series spring was considered to be a rigid link.

For a given fixed operating voltage, the torque speed relationship of direct current (DC) motors can be expressed as:

$$T_m \leq T_m^{max} - \omega \left(\frac{T_m^{max}}{\omega^{max}} \right) \qquad (4.9)$$

Where ω and T_m are the motor velocity and torque respectively. There terms T_m^{max} and ω^{max} correspond to the maximum motor torque at zero-velocity and the maximum no-load speed, respectively.

Considering a constant transmission R, the resulting output torque and velocity of the actuator are expressed as $T_o = T_m R$ and $\dot{\theta} = \omega / R$. Moreover, if we include the power output relationship $P_o = T_o \dot{\theta}$, we can define the motor bound for the power-velocity relationship.

Thus the maximum limits (bounds) of the actuator's motor-transmission system can be expressed as:

$$T_o \leq R T_m^{max} - R^2 \dot{\theta} \left(\frac{T_m^{max}}{\omega^{max}} \right) \qquad (4.10)$$

43

$$P_o \leq \dot{\theta} R T_m^{max} - R^2 \dot{\theta}^2 \left(\frac{T_m^{max}}{\omega^{max}}\right) \qquad (4.11)$$

Assuming a fixed transmission ratio of 134.8, we obtained the actuator bounds in torque-velocity and power-velocity space. The analysis was performed for average moderate-speed knee trajectories of an mid-size average male subject (Winter D. A., 1983) In the following figures, we depict the analysis results for the extension actuator.
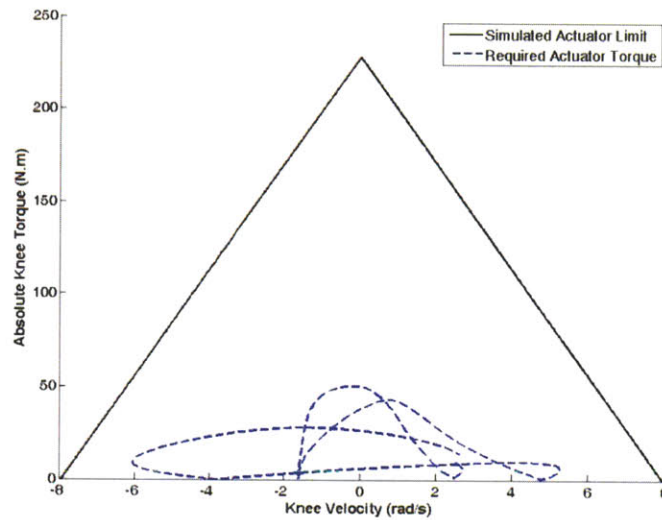
Figure 4.10- Knee torque-velocity limits for moderate walking speeds for extension and flexion actuators
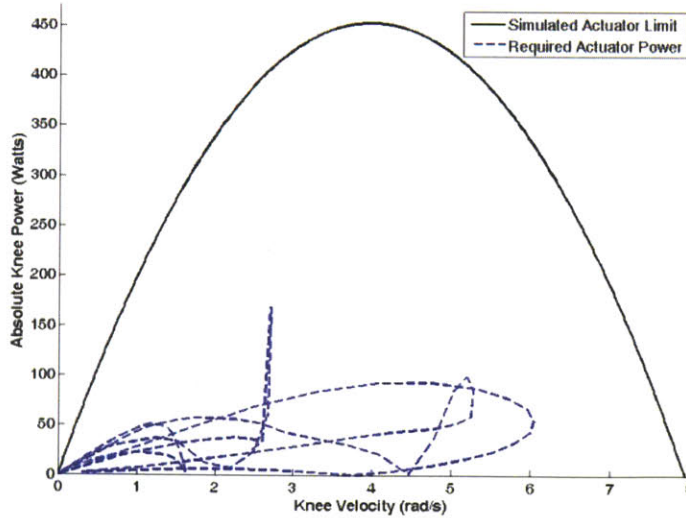
Figure 4.11-Power-velocity limits for moderate walking speed of extension actuator

44

As observed from the simulation results the biological behavior of the knee joint remains within the boundaries of the actuator limit performance, guaranteeing the knee's capability to reproduce intact knee mechanics during level-ground walking.

4.4.3 System Characterization

Model Parameter estimates

The two stage transmission used for the extension and flexion actuators have a total reduction ratio value of $R = 134.8$. The equivalent inertia M_e at the output is 0.061 kg·m^2. The reflected inertia of the motor dominates the other elements in the drive-train. The equivalent damping of the actuator and series equivalent compliance was estimated experimentally utilizing a custom built bench setup.

Bench-top setup platform

An experimental bench-top setup (figure 4.14) was designed and manufactured to characterize each of the knee actuators. The system characterization allows for the identification of the parameters in the model descriptions. This bench setup consisted of a steel rectangular base with custom attachment fixtures to rigidly secure the knee ends. These fixtures isolate the torque effect of the individual actuator on the knee joint output. The knee joint was instrumented with a commercial reaction torque sensor (FUTEK® TFF600) that measured the output torque at the joint. The electronics system of the knee and the torque sensor were connected to a mobile computer via USB in order to store the commanded currents and the electromechanical response of the knee prosthesis. Each of the sensors within the robotic knee was calibrated using the knee testing apparatus.

45
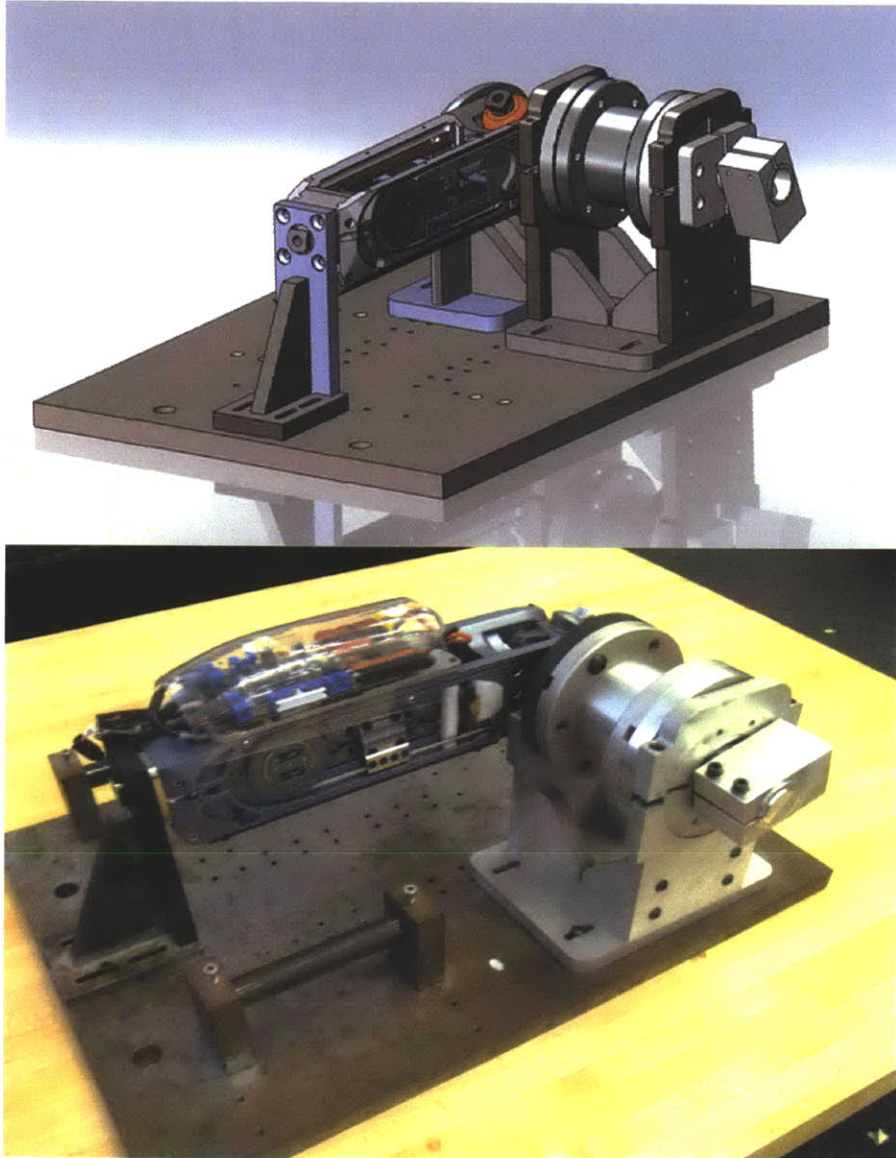
Figure 4.12-Experimental Bench-top platform setup for the active knee prosthesis.

We estimated the frequency-domain relationship between desired output torque and measured torque at the knee joint, generated by each actuator. A chirp command current was applied to the motor in the range of 0.5-20 Hz with an amplitude of 4 N.m. For safety, we limited the force output magnitude of the actuator by bounding the input current command in the range of estimated resonant frequencies would occur.

Using Matlab®'s system identification toolbox, and in particular employing the function *tfestimate*, we calculated the frequency domain relationship between the requested torque and the

measured output torque. Torque bandwith for the extension and flexion actuators is 14 Hz and 12 Hz respectively.

Both flexion and extension actuators were considered to behave as second order systems. The general model for a second order spring mass damper system is compared to the actuators' model, where the torque output relationship to the effective requested torque T_e is represented.

$$\frac{T_o(s)}{T_e(s)} = \frac{\omega_n{}^2}{s^2 + 2\zeta\omega_n s + \omega_n{}^2} = \frac{K_s}{M_e s^2 + b_e s + K_s} \qquad (4.12)$$

ω_n and ζ represent the system's natural frequency and damping term, respectively, and were obtained from the estimation of the resonant peak M_p above the steady –state zero gain:

$$M_p = \frac{1}{2\zeta\sqrt{1-\zeta^2}} \text{ and } \omega_n = \frac{\omega_p}{\sqrt{1-\zeta^2}} \qquad (4.13) \text{ and } (4.14)$$

where ω_p corresponds to the resonant peak frequency.

The frequency response curve is depicted in figure 4.13. Using these experimental results, we obtained the parameters for equivalent inertia (M_e), equivalent damping (b_e) and the effective series stiffness (K_s) through the transmission of gear ratio R for each of the actuators. These parameters were employed to simulate the frequency response of the modeled system
The series elastic stiffness is derived from the expression

$$K_s = \omega_n^2 M_e \qquad (4.15)$$

And the equivalent damping coefficient b_e can be derived experimentally from

$$b_e = 2\zeta\omega_n M_e \qquad (4.16)$$
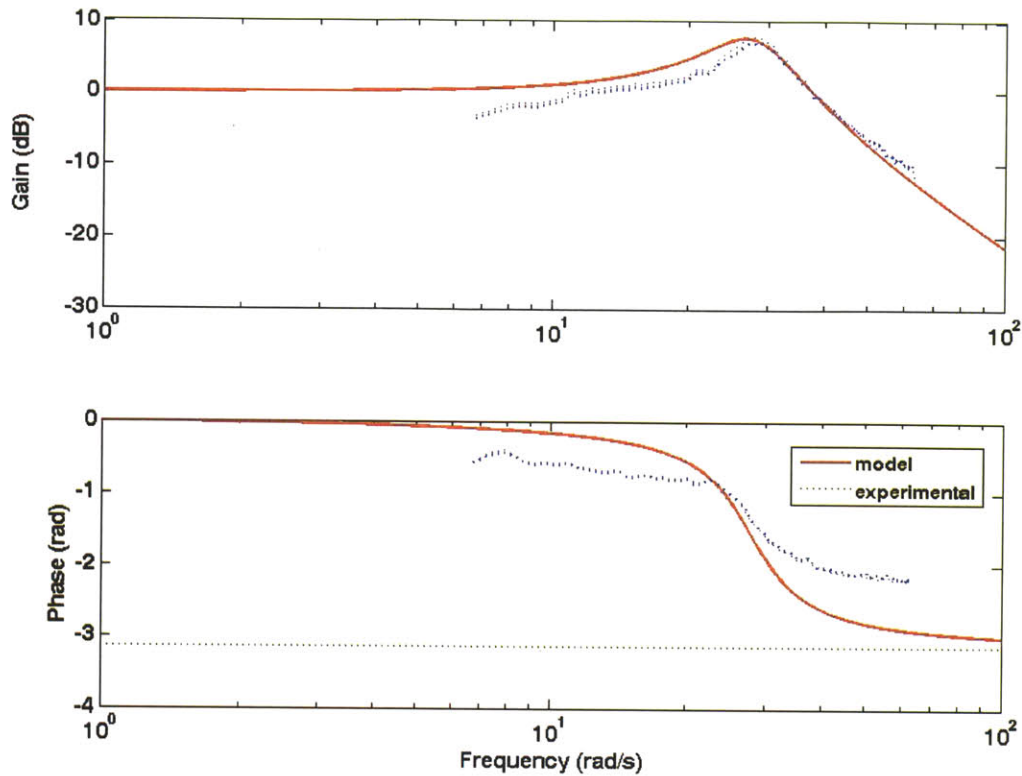
Figure 4.13-Frequency response: simulation and experimental data for the extension actuator.

For this model, we included an expected time delay (t_d) effect due to the onboard microcontroller. In the frequency domain, this delay constitutes a phase shift for the second order system. The same analysis was performed to the flexion actuator in order to determine its model parameters. The following table summarizes the set of values for the second-order system parameters that represents the extension and flexion actuators.

Actuator	Me (kg.m²)	b_e (N.m.s/rad)	K_s (N.m /rad)	t_d (s)
Extension	0.061	1.72	119	0.002
Flexion	0.061	2.13	143	0.002

Table 4.4 Extension and flexion actuator model parameters

4.5 Energy Economy

One of the features that must be considered in the design of an electrically powered prosthetic system is the amount of operation time an amputee will have before the batteries have to be recharged. At a minimum, an empirical operation time should be of one full day of normal walking activity, without the amputee having to worry about running out of battery life. Therefore, in the design of the biomimetic active knee prosthesis, the energy economy of the device is a central concern.

Energy economy is defined as an energetic cost of transport (COT) equivalent to the electrical energy required to transport a unit of bodyweight (patient and prosthesis) over a given unit distance. In particular, since the prosthesis will be tested in uni-lateral amputees, the unit of bodyweight is considered to be half of the patient's weight plus the weight of the prosthesis. These factors considered, the COT relationship can be expressed as:

Cost of Transport (COT) = Electrical energy per cycle / (distance traveled * 0.5 body weight)

For our analysis, the electrical energy required is normalized by body weight times distance traveled, assuming a heavier amputee will require a larger amount of electrical energy. This energy should cover the prosthesis' net positive work requirements that enable the device to emulate natural biomechanics for level-ground walking.

To estimate the electrical energy consumption of the prosthesis, the electrical cost of each of the motors was taken into account. A standard DC motor model was employed to estimate the energetic consumption of each actuator.

$$i_m = i_{nl} sgn(\dot{\theta}_m) + \frac{T_m}{K_t} \qquad (4.17)$$

$$V_m = \frac{\dot{\theta}_m}{K_e} + \Omega_m i_m \qquad (4.18)$$

where i_m and V_m represent the motor current and the motor voltage, respectively. K_e, K_t, i_{nl} and Ω_m are the speed constant, torque constant, no-load current and motor resistance, respectively. Thus, the power consumption of the motor can be estimated as $P_m = i_m V_m$.

For the energetic economy assessment, we used the biomechanic description of the intact knee angle-torque trajectories from chapter 3 as a reference (average mid-size male subject). In addition, we followed the general control strategy discussed in the control chapter, which describes when and how each motor is active throughout a gait cycle. Given the trajectories and active states of the actuators, we estimated the required linear motor displacement and its derivatives, including the required motor torque T_m for each of the actuators acting on the knee prosthesis during a gait cycle. We then calculated the electrical motor power consumption from the relationships in equations 4.16 and 4.17, and then proceeded to estimate the electrical energy consumption of each motor by integrating the electrical power over the gait cycle. When this energy consumption was calculated, 30% of the negative electrical energy was considered for regeneration, which can be stored in the battery and reused towards positive work power outputs. The total cost of transport for the agonist-antagonist active knee prosthesis was calculated to be $COT = 11.4$ Joules / Gait cycle

Repeating the same analysis, we compared the COT of the active knee prosthesis to two other conventional architectures that have been pursued in active prosthesis designs. These are a single series elastic actuator and a direct drive architecture, as depicted in figure 4.14 The direct drive system differs from that of the single SEA in that the series spring stiffness is removed and is replaced by a rigid link (effectively $K_s >>$). Both architectures will follow the same equations of motion as described earlier in this chapter.
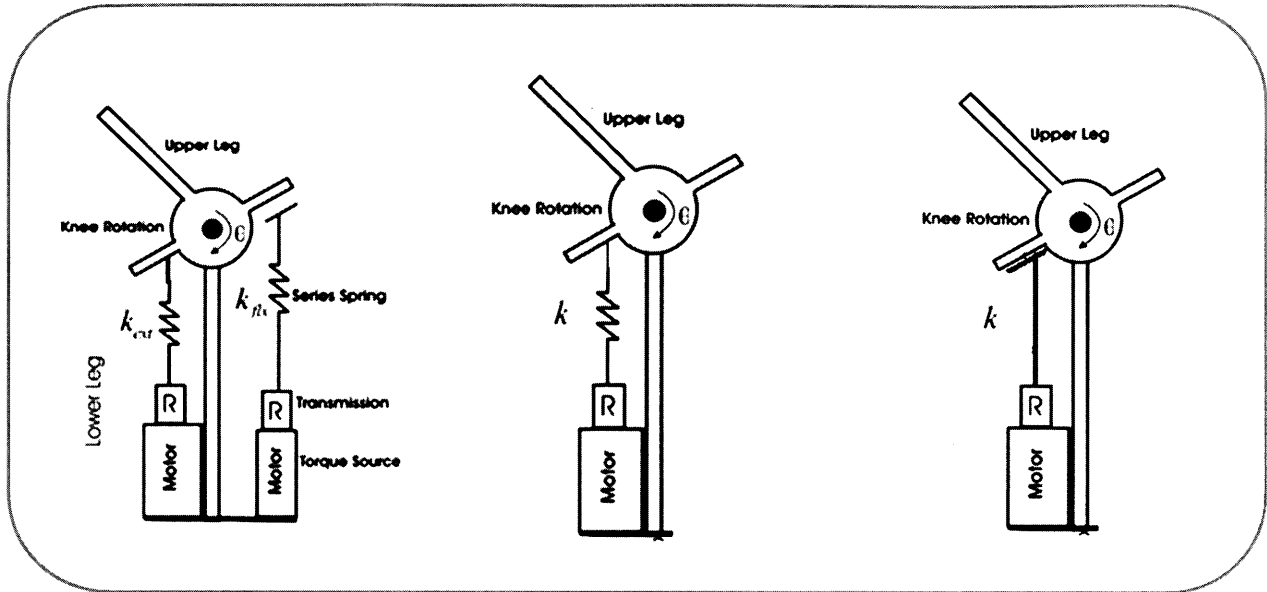
Figure 4.14 Agonist-Antagonist, Single SEA and direct-drive architectures for knee active prosthesis

The motor model equations as well as the reference biological angle-torque trajectories for an average mid-size subject (see Chapter 3), were maintained to estimate the cost of transport for each of the electromechanical architectures in the comparison. The motor selected for each of the single actuator mechanisms was the Maxon® RE40. This motor has repeatedly used for the development of electrically powered single actuator prosthetic joints for the lower leg (Au, Weber and Herr 2009) (Au, Weber and Martinez-Villalpando, et al. 2007) (Fite, Mitchell and Goldfarb 2007).The transmission ratio and series stiffness combination were selected in order to provide the minimal COT that could be achievable with such architecture, given the biological trajectory and motor selection. The same 30% of regenerative capability was employed for the single SEA and direct drive architectures.

Figure 4.15. shows simulation results for the COT of the single series elastic actuator and direct drive architecture for the active knee prosthesis for different reduction ratios and stiffness values of the series springs.

The resulting COT of these two architectures can be summarized in the following table and compared to the agonist-antagonist active prosthesis COT.

Architecture	Motor	Transmission	Series Spring	COT
Agonist-antagonist	Maxon RE30 (flexion & extension)	135	K_{flx}=137 Nm/rad K_{ext}=160 Nm/rad	11.4 J/gait cycle
Single SEA	Maxon RE40	160	Ks=128 Nm/rad	26.7 J/gait cycle
Direct drive	Maxon RE40	156	Rigid link	39.3 J/gait cycle

Table 4.5. Cost of transport comparison of active knee prostheses electromechanical architectures
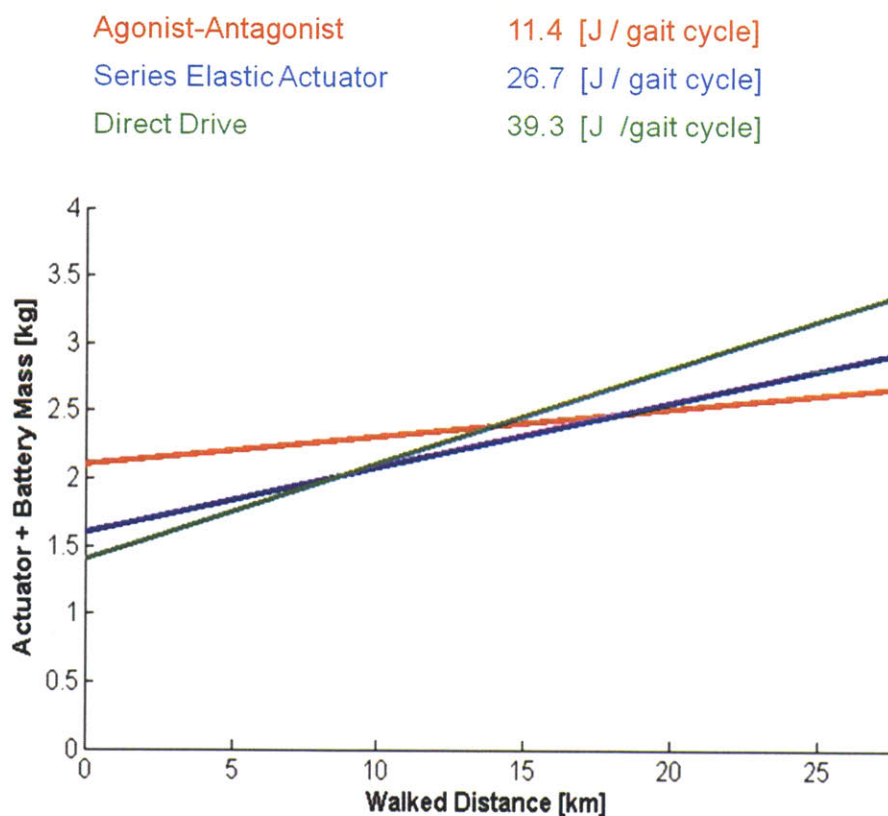
Figure 4.15- Active knee prostheses electromechanical architectures comparison. Battery mass required provided a distance traveled. At zero distance traveled, only actuator mass is considered, as walking distance increases, battery mass is required. The slope of each line corresponds to the COT for a given architecture.

Assuming that a knee prosthesis with each of these architectures is worn by a mid-size average male amputee, we estimated and compared the amount of distance the patient can walk on level-ground for a given battery mass on a single charge. Each type of prosthesis is provided

with the same battery technology for its operation, which for the purposes of this analysis is a lithium-ion battery with an energy density of 100 W.h/kg (www.a123system.com).

We assume that for each gait cycle, the amputee can walk a distance of approximately 1.5 m. Moreover, we considered that the active lower-extremity amputees walk approximately 3000 steps on average per day at a moderate speed (Stepien, et al. 2007) . Simulation results show that the agonist antagonist design becomes is desirable architecture over the other two when the desired walking distance between battery charges is more than 12 km (which is equivalent to approximately 3 days of walking). In other words, the trade-off between larger battery size and step-count makes the agonist antagonist design preferable over the other two architectures, especially if one of the design goals is to have patient walk a longer distances before require to re-charge or change the battery. This simulation just contemplates level-ground walking; however, in reality the amputee does not walk on flat surfaces only, but also performs other activities that require larger amounts of positive net power at the joint (stairs, ramps, etc). Consequently, the ambulatory capacity of the knee prostheses between battery charges becomes a fraction of the simulated values.

Chapter 5

Control

This chapter describes the control system design that enables the active knee prosthesis to emulate the intact knee biomechanics behavior during level-ground walking.

5.1 Control System Architecture

As described in Chapter 3, walking is a cyclic behavior that can be structured in several phases. These phases allow us to motivate a finite-state control strategy to direct the behavior of the active knee in walking. This general approach has been previously employed for control purposes of other locomotion assistive/prosthetic devices, including above knee prostheses (Koganezawa and Kato 1987) (Grimes 1979) (Zlatnik, Steiner and Schweitzer 2002) (Wilkenfeld 2000) (Blaya and Herr 2004).

The control system for the knee has two types of low-level servo controllers that support the control architecture of the knee. These servo controllers are a position controller and an impedance controller. The finite state machine uses local sensing information to automatically detect the gait phases and manage transitions between states. It also determines which type of low-level controller should be used to provide the adequate functionality of each of the two actuators given the control state. This type of low-level controller has been previously proposed for lower-leg powered prosthesis (S. Au 2007). The overall control system architecture is depicted in figure 5.1
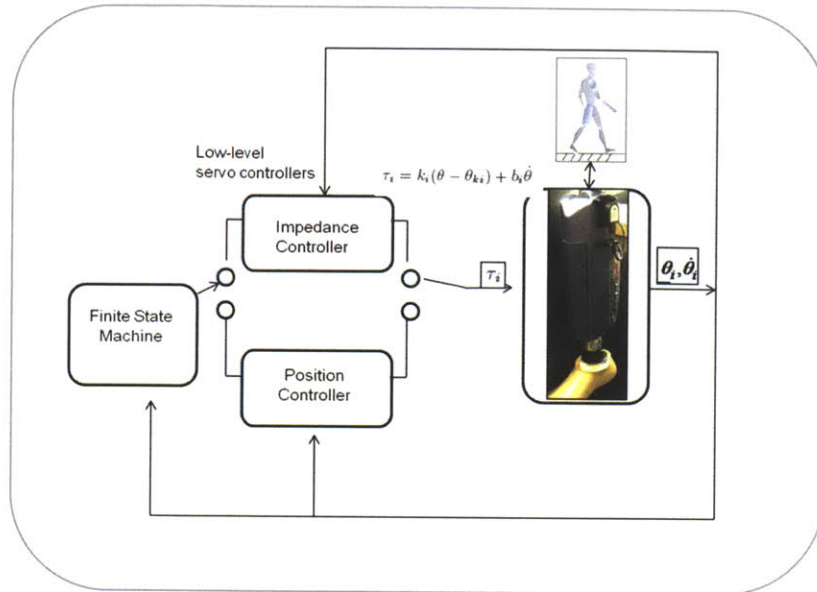
Figure 5.1-General control system architecture of active knee prosthesis
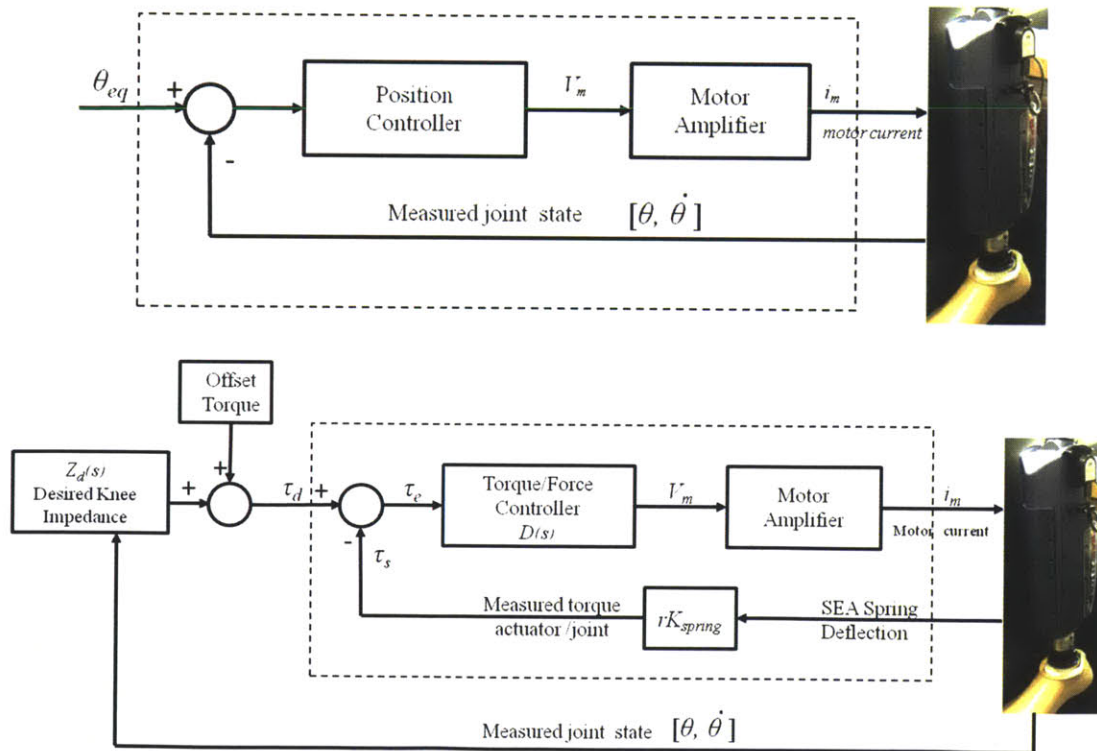
Figure 5.2-Block diagrams for low-level servo controllers

55

5.2 Low-Level Servo Controllers

5.2.1 Position controller

A PD controller is responsible for modulating the desired equilibrium position of the flexion and extension springs, $\theta_{eq} = \{\theta_{eq_{flx}}, \theta_{eq_{ext}}\}$. This controller has its use in two main circumstances. First, when the actuator behaves as a clutching component, a high gain position control is used to lock the motor shaft position in place, maintaining the desired equilibrium angle of the respective series spring. Secondly, this control is used as a position tracking control for the equilibrium point of the flexion spring element during the motion of the knee, assuring its correct location in a given state during the gait cycle. This controller can be represented as

$$V_m = K_1(\theta_{eq} - \theta) + K_2\dot{\theta} \qquad (5.1)$$

Wwhere V_m, K_1, K_2, θ are the input voltage given a desired equilibrium position, the proportional gain term, the derivative gain term, and the knee angle, respectively.

5.2.2 Impedance controller

This controller modulates the output impedance of the extension actuator that directly attaches to the knee joint via the cable transmission. This controller has two main components: an outer position feedback loop and an inner loop torque/force controller. The structure of the outer loop derives from the 'simple impedance control' architecture proposed by (Hogan 1985). This controller relies on the position/velocity feedback from the knee joint to modulate its impedance. The controller modulating the impedance of the extension series elastic actuator can be expressed as:

$$Z_d(s) = \frac{\tau_d(s)}{\theta(s)} = K_d + sB_d \qquad (5.2)$$

where τ_d, K_d, B_d are the desired output joint torque, stiffness and damping terms, respectively.

The actual output joint impedance includes both the intrinsic impedance (due to the inherent inertia and friction of the knee actuator and mechanism) and the desired output impedance due to the controller. In order to reduce the effect of the intrinsic impedance, the inner torque/force controller is incorporated into the impedance control.

The torque controller helps provide an offset torque and facilitate the impedance modulation. This controller utilizes the series spring deflection to modulate torque output from the extension SEA. This controller also follows a PD law structure.

$$D(s) = \frac{V_m(s)}{\tau_e(s)} = K_F + sB_F \qquad (5.3)$$

where τ_e is the torque error output, V_m is the input voltage command, and K_F, B_F are the proportional and damping terms, respectively. Using this torque controller along with the open loop model with fixed-load condition as expressed in Chapter 4, we can obtain the close loop transfer function between actuator output torque τ_s and desired torque τ_d (that can be expressed in terms of a input voltage command). These actuator torques have a corresponding linear force F_s, F_d that affect the joint impedance as expressed in the mechanical analysis of chapter 4 . The transfer function can be expressed as

$$\frac{\tau_d(s)}{\tau_s(s)} = \frac{(K_F + sB_F)K_{total}G}{1 + (K_F + sB_F)K_{total}G} \qquad (5.4)$$

where K_{total} is the transmission ratio R multiplied by the motor constant and amplifier gain, corresponding to the term that allows the conversion from commanded voltage to commanded force. This control includes a tunable fixed gain G. The constant terms in this controller were chosen experimentally (i.e. using standard root-locus technique) to achieve an adequate of 10 Hz which surpasses 2 Hz motion bandwidth set a as design specification.

5.3 Finite State Controller

A finite state controller for level-ground walking was implemented to emulate the intact knee behavior during level ground walking. The three basic states of the controller are (i) Stance, (ii) Swing-Flexion, and (iii) Swing Extension. In general terms, a quasi-passive equilibrium point control was implemented in the Stance, and an impedance control (variable-damping) in the Swing states. Transitions between states were determined primarily by four sensor information variables: heel ground contact, toe ground contact, knee angle and knee torque. The finite state control diagram indicating transitions is shown in figure 5.3.
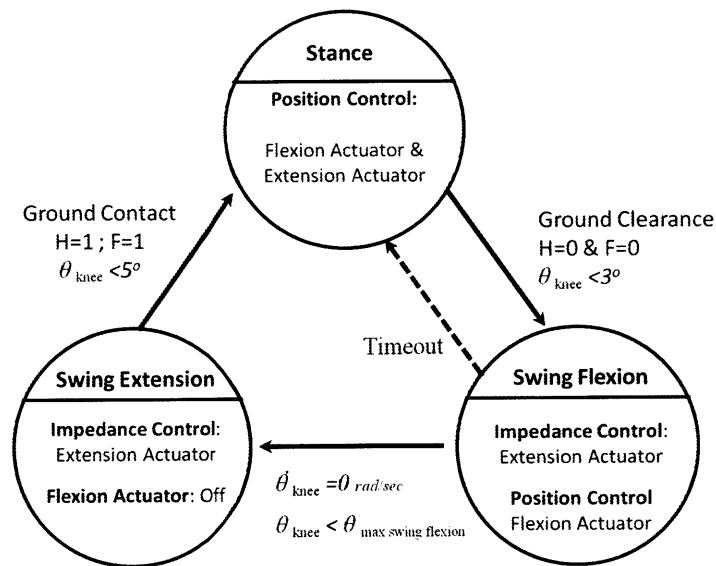
Figure 5.3-Basic finite- state machine controller for level-ground walking. Three basic states are shown with control actions and transitional conditions. The states are *stance, swing flexion*, and *swing extension* .

For state identification and transitions, the controller relied on the following variables:

Heel contact (H). H=1 indicates that the heel is in contact with the ground, and H=0 indicates the off-ground status.

Forefoot contact (F). F=1 indicates that the forefoot is in contact with the ground, and F=0 indicates the off-ground status.

Knee angle (θ) is the relative angle of the knee joint. All knee angles are flexion angles. Angles θ_E and θ_F define the angles at which the extension and flexion springs become engaged during stance, respectively. Further, θ_+ is the angle of the knee during swing flexion, and θ_- is the angle of the knee during swing extension.

Knee torque (τ) is determined using the series-spring compression and measured using the encoder information from the actuators and knee joint.

Each of the three states and the corresponding actuator behavior is described in the following section.

(i) *Stance*. At the start of the gait cycle, as the heel makes contact with the ground (H=1), the extension actuator is "locked" using a high gain position control with a desired motor velocity equal to zero. This action effectively corresponds to clutching the extension series spring elements. The engaged series compliance has a set equilibrium angle corresponding to the knee joint angle at heel strike θ_E. During early stance knee flexion (knee torque $\tau < 0$), the extension spring stores energy in preparation for stance knee extension.

During stance knee flexion, the equilibrium point of the flexion spring θ_F is commanded via position control to closely track the linear carriage linked to the knee output joint. When the knee has reached its maximum flexion angle in stance, the knee rotation changes and begins to extend, and at this point the flexion motor stops tracking. The flexion spring then becomes engaged (effectively clutched) with a spring equilibrium angle equal to the knee's position at maximum knee flexion θ_F., The electrical cost of maintaining the flexion spring's position is zero, due to the lead-screw's lack of back-drivability. During change of flexion to extension motion in stance, there is an energy exchange between the actuators' series springs. Energy stored in the extension spring assists knee extension in addition to contributing to the energy stored in the flexion spring.

As the heel lifts off the ground (H=0), while the forefoot is still on the ground, the knee angle is reduced as the knee starts extending again in *Pre-Swing* ($\theta < 3°$). The energy stored in

the flexion spring assists knee flexion in preparation for toe-off. The flexion actuator holds the engagement of its series spring. When previously stored energy in the extension spring is dissipated, the equilibrium point of the extension spring θ_E is controlled with zero impedance, allowing the knee to flex in preparation for the swing phase.

(ii) *Swing Flexion* begins at toe off (T=0). The extension actuator is controlled under zero torque impedance control to allow for swing flexion. Energy from the flexion spring assists in the knee flexion after toe-off. Immediately after that energy has been spent, the flexion actuator is position controlled to servo the flexion spring (under no load) to its neutral position before heel strike. The extension actuator is now the actuator in charge of modulating the behavior of the knee joint.

As the knee flexes beyond 20 degrees ($\theta_+ > 20^\circ$), a damping control is implemented with the impedance controller. Specifically, a low gain damping control on the extension actuator acting as a variable damper reduces hyper-flexion of the knee until it reaches zero velocity at maximum swing flexion angle. The knee reaches approximately 60 degrees ($\theta_+ \sim 60^\circ$), and the knee changes motion into swing extension.

(iii) *Swing Extension*. After reaching maximum flexion in swing, the knee begins to extend, and the extension actuator is impedance controlled as a variable damper to decelerate smoothly the motion of the swinging leg in preparation for the heel strike of the subsequent gait cycle.

During swing extension of healthy intact subjects, the biomechanical behavior of the knee joint in level-ground walking reveals a variable damping profile that varies with respect to joint angle. This behavior has two distinct phases that can be characterized by a linearly increasing damping profile through early swing extension, and a non-linear damping behavior in late swing. The latter can be approximated through a quadratic function. In figure 5.4 the average damping coefficient during swing extension for ten healthy subjects walking at self-selected speeds is shown. Data from the study presented in (Herr and Popovic 2008) was used to obtain the information in this plot.
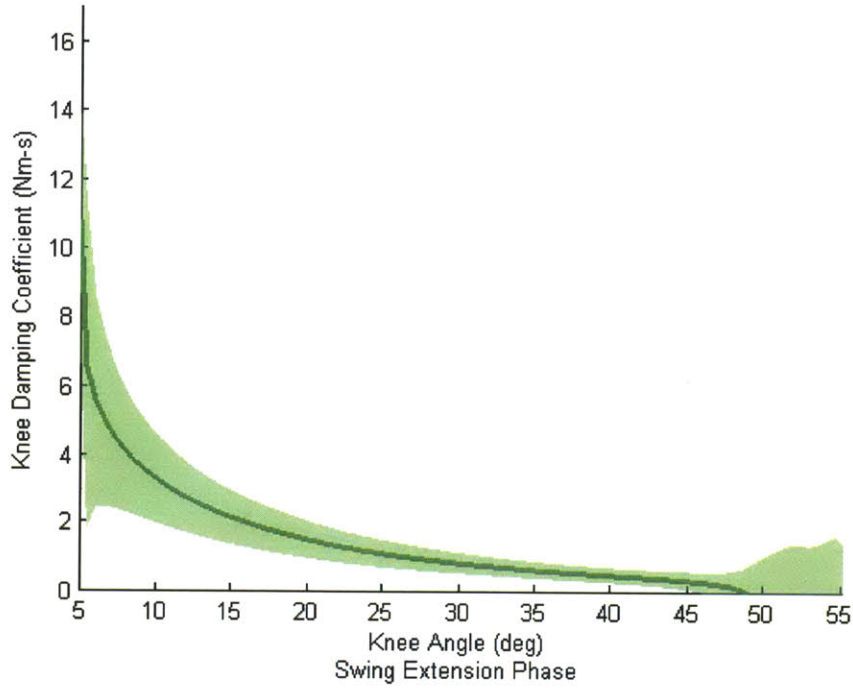
Figure 5.4-Knee damping coefficient during swing extension for able-bodied subjects walking at self-selected speeds. Solid line represents average data and the shaded region is within one standard deviation from the mean

The two damping phases (linear and quadratic) are implemented in the impedance controller as a piece-wise functional dependent on the prosthesis' knee angle.

$$B_d(\theta) = \begin{cases} \dfrac{B_0 - B_T}{\theta_0 - \theta_T}(\theta - \theta_T) + B_T & : \theta > \theta_T \\ \dfrac{B_1 - B_T}{(\theta_1 - \theta_T)^2}(\theta - \theta_T)^2 + B_T & : \theta \leq \theta_T \end{cases} \qquad (5.5)$$

where B_d is the desired joint damping coefficient as part of the impedance controller in equation 5.2. The constants θ_0, θ_1 are angle constants determined experimentally and are equivalent to 50° and 5°, respectively. B_0, B_1 and B_T are intial, terminal and transition damping terms that we experimentally tuned for swing extension controller while evaluating the performance of the knee joint during experimental trials. θ_T corresponds to the transition angle between the linear and the non-linear damping profile. The proposed swing-extension damping control for knee

61

prostheses and its implementation on single-subject walking tests are presented in (Mooney 2012).
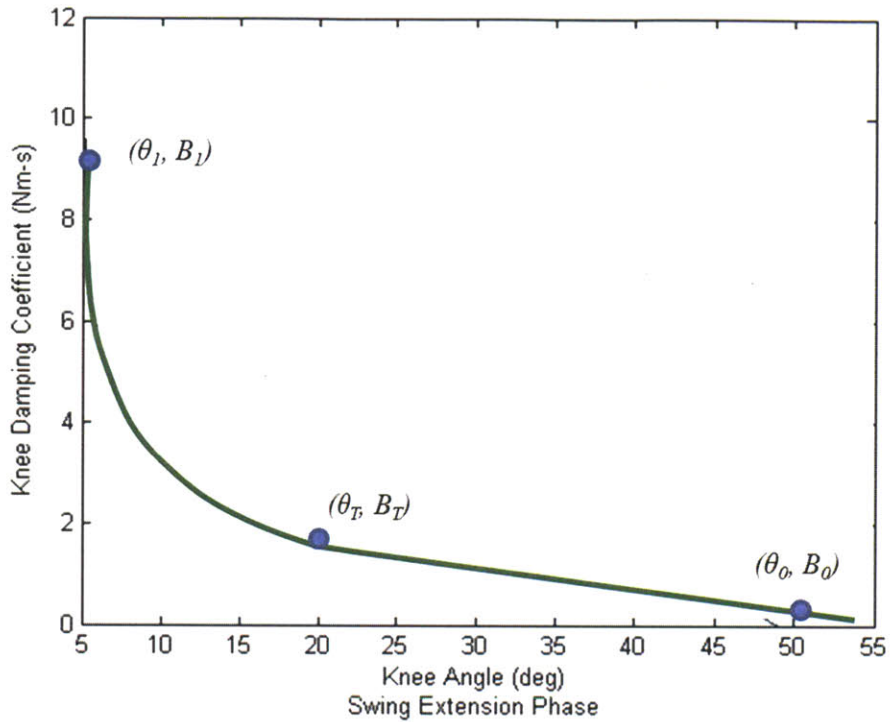
Figure 5.5-Variable damping profile of the knee joint during swing extension using piece-wise approximation to biological reference trajectory.

The active knee takes advantage of the incorporated series-elastic components in combination with the variable-impedance control to minimize the electrical energy demands during walking. With the combination of mechanical design architecture and control, the prosthesis' electrical motors do not perform positive work on the knee joint during level-ground walking, resulting in modest electrical power requirements. With this strategy the knee behavior can emulate intact knee mechanics.

5.4 Sensors

Feedback to the controller was provided by onboard intrinsic sensors. In particular, position and compression for each series spring were monitored, as was the knee angular position. Knee torque was calculated indirectly using the spring deflections. Ground contact was measured

utilizing an instrumented insole placed inside subject's shoe and wired to the onboard electronics system. All electronics were implemented on a single board mounted on the knee chassis installed on posterior face of the knee. Motors were driven by direct current H-bridge controllers with speed governed by 20 kHz pulse width modulation (PWM) and powered by a six cell Lithium polymer battery (22.2V nominal). Analog sensors were read through a 10-bit analog to digital converter (ADC). The system was controlled by an AVR microcontroller and could be monitored by either USB or Bluetooth. Because all processing was done onboard and power was supplied by a relatively small lithium polymer battery (mass=0.16 kg), the prototype was completely self-contained and did not require tethering.

Measurement	Sensor	Part number
Knee angle	Digital encoder	US Digital® S1-1024-236
Motor rotation	Digital encoder	Maxon® MR 500
Spring compression	Encoder differential	N.A.
Heel / Toe contact	FSR foot switch	B&L Engineering® FSW -9
Orientation / acceleration	Accelerometer / gyroscope (3 axis)	ADIS16006 & ADIS16100

Table 5.1. Sensors for the active knee prosthesis

5.5 Onboard Computer System

The knee has a custom made electronic system based on AVR microcontroller technology. The knee's custom electronics design by G. Elliott is based on the system implemented in (Elliott 2012). This electronic system's allows for autonomous (non-tethered) control and monitoring of the active knee prosthesis as the subject ambulates. The series of features of this board are depicted in the following table.

63

System	Dimensions	10.2 x 6.4 x 1.8 cm
	Firmware	LegOs 4.4 (custom)
	Update Frequency	1 kHz
	Debugging	Onboard USB 14 Hr data log Connection to external serial device
Outputs	Motor Controllers	2x 10A continous, 20A peak brushed controller with 9-bit speed control 2x Current sensing with 12-bit resolution and ±30A full scale 2x User-replaceable fuse
	Indicators	6x User controllable LED with 8-bit PWM 2X Motor state LED (RGY) with 8-bit PWM
Inputs	Encoder Counters	2x Differential encoder counter with programmable index 2x Single-ended encoder counter with programmable index
	Analog Inputs	4x High impedance unity gain 10bit input with programmable anti-aliasing filter; configurable 2nd order Butterworth or Bessel with cutoff freq. 20-500 Hz 2x High Impedance programmable gain 12bit differential input with gain from 20-1000 or 11-bit single ended input with gain 1-40 with 300Hz 8th order elliptic anti-aliasing filter
	Inertial inputs	Onboard 3-axis accelerometer with 12 bit resolution and programmable ±2g or ±6g full scale Onboard 3-axis gyroscope with 16 bit resolution and programmable ±250°/s, ±500°/s or ±2000/s full scale
	Time Keeping	Real time clock
Battery Management	Battery Protection	Under-voltage lockout for 3 -6 cell lithium polymer packs User-replaceable fuse
	Battery Charger	1A charger for 3-6 cell lithium polymer packs
Other	Daughterboard	2x connection to external auxiliary device

Table 5.2. Features of the electronic suite system for the active knee prosthesis
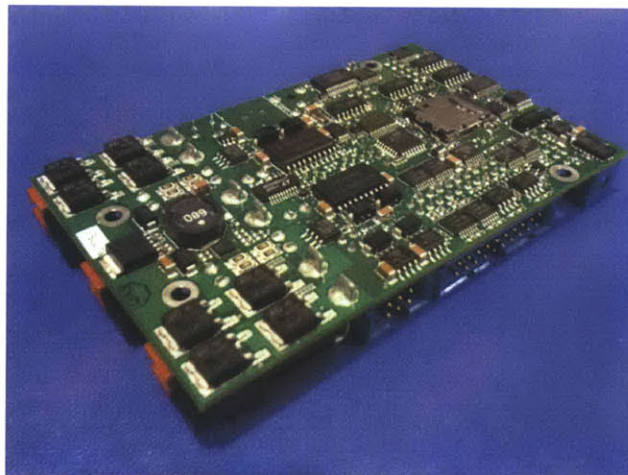
Figure 5.6-Circuit board assembly of new electronic system main board

Startup

Initialize System State

Initialize Interfaces

Hardware Initialization

Initialize Extension Motor / Encoder

Initialize Flexion Motor / Encoder

Initialize Knee Encoder

Initialize Foot Pad Insole

Initialize LED Drivers

→ Bootloader

Latch In

Read Extension Encoder

Read Flexion Encoder

Read Knee Encoder

Read Foot Insole/ Ground Contact

→ Soft Kill

→ Hard Kill

User Space

Lead In

Calculate Encoder Differentials

State Machine

Power On

Sleep

Stance

Position Control:

Flexion Actuator &
Extension Actuator

Ground Contact
H=1 ; F=1
$\theta_{knee} < 5°$

Ground Clearance
H=0 & F=0
$\theta_{knee} < 3°$

Timeout

Swing Extension

Impedance Control:
Extension Actuator

Flexion Actuator: Off

Swing Flexion

Impedance Control:
Extension Actuator

Position Control
Flexion Actuator

$\dot\theta_{knee} = 0 \ rad/sec$

$\theta_{knee} < \theta_{max \ swing \ flexion}$

→ Soft Kill

Lead Out

Update Close Loop Controllers

→ Hard Kill

Latch Out

Update Motors Sates

Update LED Drivers

→ Soft Kill

→ Hard Kill

Debugger

Fetch Debug Data

Packetize and Transmit

→ Hard Kill

Remote Control

Process Receiver Buffer

→ Soft Kill
→ Wake
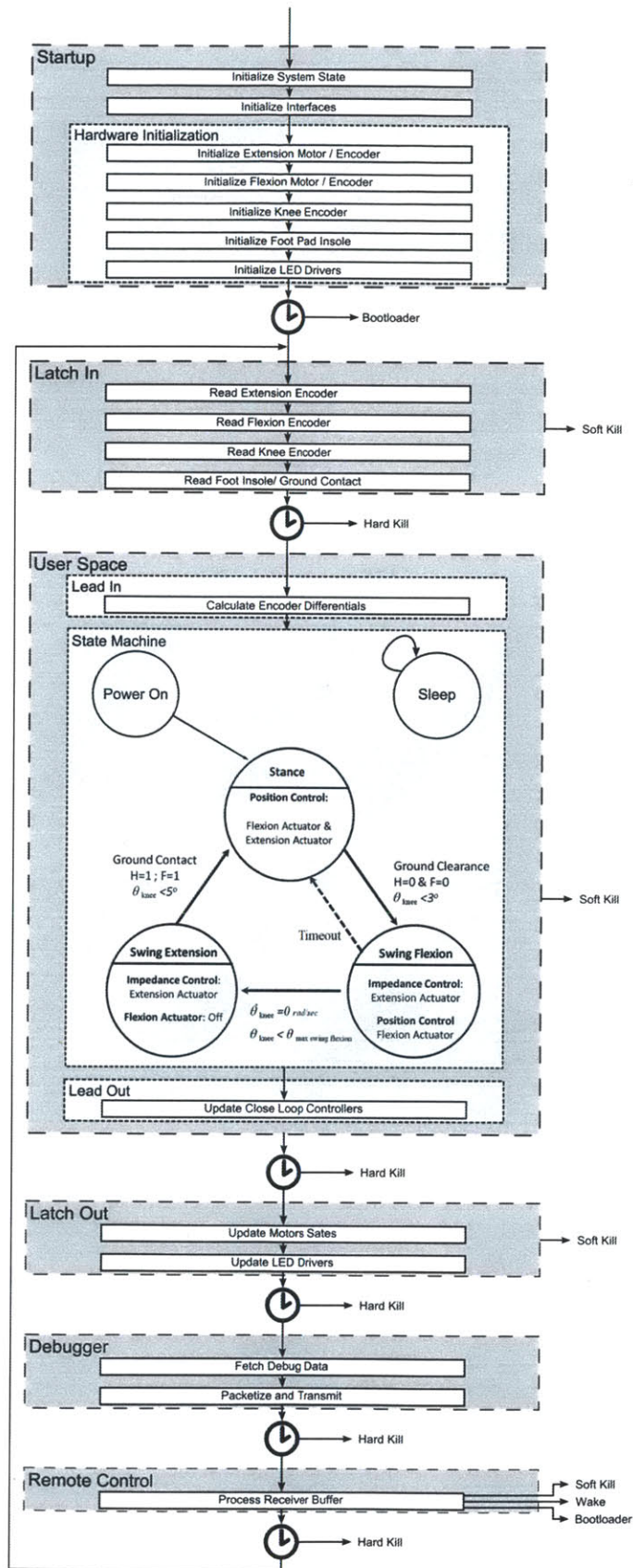→ Bootloader

→ Hard Kill

Figure 5.7-Program flow through the control framework for the active knee prosthesis.

The firmware for this system is written for the AVR ATMega*8 line of microcontrollers. It provides a synchronous read-out of all sensors and updates of all output devices. It also gives the end user diagnostic and remote control capabilities, and it is designed so that the space accessible to an end user is easy to develop. The framework in this system has the following phases of operation:

- Latch In: All input devices are read into memory.
- User Space: A state machine is updated based on newly updated input data. Lead In and Lead Out sub-phases are executed immediately before and immediately after the state machine's update and are suited for filtering inputs and updating closed-loop controllers independently of the current state.
- Latch Out: Changes made to output devices during the User Space phase are applied to hardware.
- Debugger: A programmable set of data is logged, usually to USB or onboard memory.
- Remote Control: A programmable set of memory locations may be updated, usually over USB. The remote control also provides for remote soft 'disable' and 'wake' as well as access to a *bootloader* so that new system code may be loaded. Time division is enforced by a timer interrupt, and a timeout results in an immediate hard kill, in which all potentially hazardous outputs are turned off and the system is shut down pending a reset via physical input or the remote control.

The onboard electronics system allows for the active knee prosthesis to be worn without the need of tethering to a computer or power supply. This autonomy is advantageous towards the clinical evaluation with amputee subjects, improving overall mobility, reducing the effect of external wiring interference to their gait and minimizing the risk of tripping over tethering communication and/or power cables.

Chapter 6

Clinical Evaluation

6.1 Preliminary able-bodied subject testing

Prior to evaluating the active knee prosthesis with a group of unilateral transfemoral amputees, we tested the device with an able-bodied subject utilizing a custom kneeling socket prosthesis adaptor. This evaluation was performed with amputees' safety in mind, with the dual purpose of ensuring that the prosthesis was capable of emulating intact knee biomechanics and that the finite-state machine controller functioned adequately in continuous level-ground walking.

For this test, the prosthesis was worn by an 81 Kg, 1.76 m tall able-bodied subject using a leg-amputation simulator.. The subject walked within parallel bars on a zero-incline treadmill at three different speeds (0.9, 1.1 and 1.3 m/s) for a duration of five minutes at each speed. The subject wore a kneeling socket adaptor which enables walking on the prosthesis and simulates amputee walking, facilitating development of the control strategy and fine-tuning of the control parameters. The kneeling socket device is a modified commercial hands-free crutch (i-Walk Free®). Using the onboard sensors and electronics system, we recorded joint angle and torque as well as state machine

Figure 6.1- Able-bodied wearing active knee prosthesis using kneeling socket.

In this preliminary evaluation with an intact able-bodied subject, the active knee prosthesis demonstrated the ability to provide qualitative agreement with intact knee biomechanics during level-ground ambulation at different walking speeds in the controlled treadmill study. Figure 6.2 depicts the average angle vs. torque curves at the knee joint for each walking speed. These results suggest that the antagonistic architecture in coordination with the variable-impedance control can facilitate step to step adaptation to speed variation during amputee locomotion. This architecture and controller take advantage of the passive dynamics of the artificial limb in order to replicate the biomechanics of an intact knee joint.
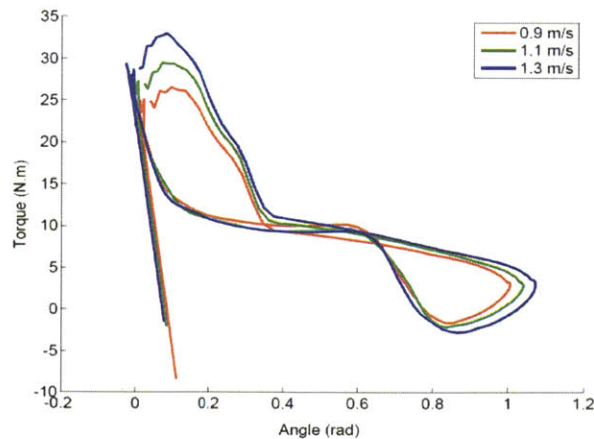

Figure 6.2-Average angle vs torque curves of the active knee prosthesis during treadmill walking of able-bodied subject using kneeling-socket adaptor.

Figure 6.3 exemplifies controller state transition performance for three consecutive, level-ground walking cycles of the implemented controls strategy in embodiment. The control states for level-ground walking are defined as follows: *Stance* (state 1), *Swing Flexion* (state 2), and *Swing Extension* (state 3).
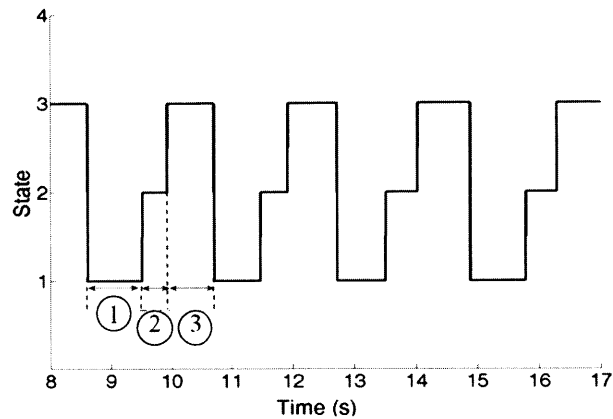

Figure 6.3-Scope of the active knee finite-state control transitions during level-ground walking. The controller robustly transitions through the finite state machine during the five minutes of consecutive walking cycles. The states are *Stance* (state 1), *Swing Flexion* (state 2), and *Swing Extension* (state 3).

6.2 Evaluation of the active knee prosthesis with transfemoral amputees

For this investigation, we hypothesized that the biomimetic agonist- antagonist active knee prosthesis with a variable-impedance controller can provide a metabolic economy advantage compared to commercial mechanically passive and variable-damping prosthetic knee devices at self-selected walking speeds. Moreover, we hypothesized that this metabolic advantage is a consequence of significant differences in gait biomechanics that result from distinct ambulatory strategies that amputees develop when wearing the active knee prosthesis. In order to begin testing these hypotheses, we recruited a group of four unilateral transfemoral amputees for clinical evaluation. In this evaluation, we measured the metabolic demand of walking and analyzed the kinematic and kinetic effects of both the active knee and the prescribed prostheses at self-selected speeds.

6.2.1 Data collection and experimental protocol

Four unilateral subjects with unilateral above-knee amputations participated in the study. The experimental protocol was approved by MIT's institutional review board (Committee on the Use of Humans as Experimental Subjects, COUHES). Before participating in the study, each subject provided written informed consent as established by the protocol. At any time during the study, subjects were able to withdraw.

The transfemoral amputees recruited to participate in the study were experienced at walking with prostheses, with a capacity of locomotion at least at a K3 level (i.e., having the ability or potential for ambulation with variable cadence). Participants were considered healthy with no other musculoskeletal problems or any known cardiovascular, pulmonary or neurological disorders.

Subject	Gender	Height [cm]	Mass [kg]	Affected leg	Prescribed knee prosthesis	Prescribed Ankle-foot prosthesis
1	Male	182	98.7	Right	Otto Bock C-leg®	Otto Bock Trias®
2	Male	180	97.5	Right	Endolite Mercury®	Endolite Elite®
3	Male	179	77.1	Right	Otto Bock Genium®	Otto Bock Trias®
4	Male	181	99.8	Left	Ossur Rheo®	Endolite Elite2®

Table 6.1. Amputee participant characteristics

For each amputee participant, a complete study included three separate experimental sessions. Each session took place at a different location at the MIT campus. In the first session the amputee was fitted with the active knee prosthesis by a certified prosthetist. This session also allowed the investigator to certify the amputee's K3 locomotion competence with the active prosthesis and to ensure the patient was able to complete the other two sessions at minimal risk. The goal of the second session was to assess the impact of the active knee prosthesis on the transfemoral amputees' metabolic cost of ambulation. This session took place at an indoor athletic track so that the amputees could walk at self-selected speeds. Finally, the third session was performed at a motion analysis laboratory so that we could study the differences in

kinematics and kinetics associated with the use of the active knee prosthesis as compared to the amputees' prescribed prosthetic system. The evaluation order for the second and third sessions could be changed depending on amputees' availability as well as laboratory space use timing constraints.

The locations for the three sessions were the MIT Biomechatronics research space at the MIT Media Laboratory, the indoor track at MIT's Johnson Athletic Center, and the motion capture and gait laboratory at MIT's Computer Science and Artificial Intelligence Laboratory (CSAIL). Each session took an average of three hours to complete with an average time between experimental sessions of approximately one to two weeks, depending on amputees' availability.

Before testing took place in any session, the active knee prosthesis and conventional prescribed prosthetic systems were fitted by the same certified prosthetist. Alignment and fitting were consistent across all experimental sessions. Each patient used his prescribed prosthetic socket and prosthetic foot during the testing of both knees (active and prescribed). To maintain consistency, patients also wore the same pair of shoes for all experimental sessions.

First session. Subjects were fitted the active knee prosthesis and were given about one hour to get acclimatized to the device walking between 10-m parallel bars (for added safety). During the fitting process and acclimatization period, the control parameters of the active knee were tuned. After the acclimatization period, each subject was asked to walk along the 10-m level walkway at a comfortable self-selected walking speed with the active knee and then with their conventional (prescribed) prosthetic systems. Ten walking trials were performed with each of the two prostheses. Self-selected speeds for each condition were recorded and compared.

Figure 6.4-Fitting of active knee prosthesis. Adequate alignment with laser guide. Location: Biomechatronics research group at MIT Media Laboratory.

Second session. We assessed the metabolic cost of walking by measuring rates of oxygen consumption and carbon dioxide production with a lightweight portable cardiopulmonary exercise system (Cosmed K4b2, IT). Before the assessment, the self-selected walking speed was confirmed. The participant was asked to walk around the track for eight minutes with his conventional knee prostheses at the comfortable self-selected speed, in order to establish a control metabolic rate when walking. After resting for ten minutes, the patient was fitted with the active prosthesis and allowed to get acclimated to the device by walking on it for five to ten minutes. He then walked around the track for eight minutes with the active knee while gas exchange rates were measured
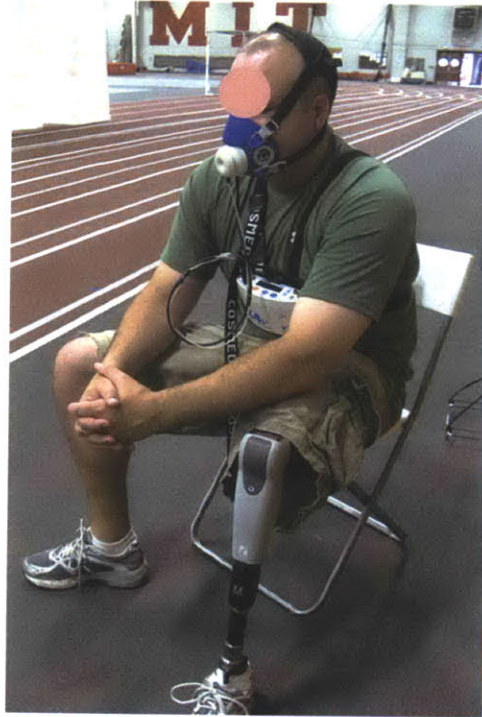
Figure 6.5-Unilateral above-knee amputee instrumented with portable K4b2 telemetric system equipment for metabolic cost assessment.

To maintain a constant self-selected walking speed during the trials using the prescribed and active knee prosthesis, the patient was instructed to follow and maintain the pace of an electric vehicle programmed to move at the same self-selected speed. Resting gas exchange rates were measured with the participant seated for five minutes before the walking trials to establish a basal metabolic control measurement.

Third session. Kinematic and kinetic data were collected at the motion capture and gait laboratory. The amputee's kinematic data was computed by measuring 3-D positions of reflective markers placed at specific body landmarks. After instrumenting and fitting each patient with the prosthesis, we gave the patient a five to ten minute acclimatization period. Then, each patient was asked to walk along a 10 m level walkway at a self-selected speed. Ten walking trials with each of the two prostheses were recorded. Kinetics were computed from measurements of ground reaction forces derived from force plates (AMTI, Inc. MA) embedded in the walkway. Joint biomechanic measurements were calculated based on a standard

biomechanics model, taking into consideration the different inertial parameters of the affected limb.

Figure 6.6-Transfemoral amputee wearing the biomimetic active knee prosthesis, instrumented with reflective markers at the motion capture laboratory .

6.2.2 Data processing and analysis

To measure the impact on the amputees' metabolic cost of ambulation, the subjects' breath-by-breath pulmonary gas exchange data were collected at the indoor track walking session. Data were recorded using a portable cardiopulmonary exercise testing system (Cosmed K4b2, IT). Volume rates of oxygen consumption and carbon dioxide production were used to estimate metabolic power cost during four minutes of steady state walking. Average gas volumes during steady state walking were used to estimate the metabolic power $P_{metabolic}$ for each walking trial using the well documented (Brockway 1987) expression:

$$P_{metabolic} = 16.48*V_{O2} + 4.48*V_{CO2} \qquad (6.1)$$

V_{O2} and V_{CO2} correspond to the average volume rates of oxygen inhalation and carbon dioxide exhalation in liters [L]. The constants 16.48 and 4.48 are established conversion rates in units of kilowatt per liter kW/L (Brockway 1987).

The net metabolic power associated with each condition was calculated by obtaining with equation 6.1 and then subtracting the calculated average resting power. The net metabolic power was then normalized by body-weight for each of the participants and compared for all subjects. Results were analyzed using pair wise two sided t-test comparisons to identify significant differences between the two experimental conditions (wearing the active knee prosthesis and wearing the prescribed prosthesis). In order to consider indication of a trend, P values between 5 and 10% were considered. Significance at a 5% level was established for this evaluation within a given subject.

The kinematic and kinetic data were collected using a motion analysis system (Vicon 512) recording at 120Hz. Kinematics were derived measuring the spatial locations of passive reflective markers adhered to amputees' body as defined a modified Helen Hayes biomechanical model marker set. Critical reflective markers were placed at the following body landmarks: forefeet, heels, lateral malleoli, lateral femoral condyles, anterior superior iliac spines, sacrum, C7, and also included shoulders, elbows and wrist. The set included also four head markers for

reference. .Joint and body kinematics and kinetic trajectories were computed in combination with measures of ground reaction forces (GRFs) from two staggered instrumented force platforms (AMTI BP-600900) embedded in the walkway. Forceplate data was sampled at 960 Hz. Inverse dynamic calculations were performed utilizing commercial software SIMM 5.0 by MusculoGraphics ® Different inertial properties inherent to the affected extremity were considered, for the different prosthetic system technologies under investigation. Biomechanic features of the patient in locomotion using each of the investigational prostheses (prescribed and active) were estimated and compared using custom software developed in MATLAB®. Results were analyzed using pair wise two sided t-test comparisons to identify significant differences among the two experimental conditions (wearing the active knee prosthesis and wearing the prescribed prosthesis). As an indication of a trend, P values between 5-10% were considered. Significance at a 5% level was established for this evaluation within a given subject.

Chapter 7

Results and Discussion

7.1 Walking speed

For each of the walking trials at the motion capture and track facilities, the self selected speed of each subject using the active knee remained within 5% of their selected average speed when wearing their prescribed system. Average self selected speeds of each of the participants in the study tended to increase when they wore the active system as compared to when the subjects wore their prescribed prosthetic knee. However, data do not provide sufficient statistical evidence to present a trend or significant difference when taking into account all subjects. Average electrical power consumption of the knee was approximately 11 ± 3 W / gait cycle.

During the walking trials, patients expressed that they felt they could walk faster if needed, and that doing so would be easier with the active knee. In contrast, the feeling of 'sluggish' behavior was a common description of patients when they returned to the use of their prescribed system after wearing the active agonist antagonist prosthesis. This empirical feedback from patients suggests that there is an inherent 'felt' benefit of using the active knee for locomotion at faster speeds. This can serve as a basis to evaluate further the performance of the active prosthesis at faster (non-self selected) speeds, including its clinical impact on metabolic and biomechanics.

Subject	Prescribed knee	Average walking speed [m/s]	
		Using the prescribed knee	Using the active knee
1	C-Leg	1.28±.03	1.34 ±04
2	Mauch	1.36±.03	1.38±.03
3	Genium	1.36±.03	1.40±.02
4	Rheo	1.28±.03	1.36±.07

Table 7.1. Self-selected walking speeds with prescribed and active knee prostheses.

7.2 Metabolic cost of walking

The metabolic cost of walking for each of the subjects was calculated using equation 6.1. and then normalized by bodyweight. These results take into account resting metabolic power and reflect four minutes of steady state walking at the athletic track with the prescribed and active knee prostheses. All four subjects in the investigation showed a metabolic cost reduction when wearing the active knee prosthesis. The use of the active knee prosthesis showed a maximum reduction of 9% for the subject with the prescribed *Mercury* knee prosthesis (subject #2). The smallest metabolic reduction observed was with subject #3 (with prescribed *Genium* prosthesis, which is considered the most advanced of the variable damping knees in the study). The subjects wearing the other two variable damping knees (*C-leg* & *Rheo*) showed similar metabolic cost reduction results of 6.5% and 6.8%. The average metabolic reduction above resting, considering all subjects, was 5.8 %. These results reflect a trend of metabolic cost reduction as a result of wearing the active knee prosthesis versus the commercially prescribed knees (variable-damping and mechanically passive) tested with a value $P=0.055$.

To the best understanding of the author, this is the first time that the use of an active knee prosthesis attached to a passive foot-ankle system has shown a metabolic cost reduction when compared to conventional prostheses. In order to provide sufficient statistical evidence to support significant differences in the effect of the active knee on metabolic cost of walking, more transfemoral amputees are to be included in a continuing study.

Subject	Prescribed knee	Metabolic Power [W /kg]		Reduction (%)
		Walking with prescribed knee	Walking with active knee	
1	C-Leg	6.3±0.1	5.9±0.1	6.5
2	Mauch	5.1±0.1	4.7±0.1	9.0
3	Genium	6.5±0.1	6.4±0.1	1.0
4	Rheo	5.8±0.1	5.5±0.1	6.8
			Average	5.8

Table 7.2. Metabolic cost of walking of four transfemoral amputees walking on level-ground at self-selected speed using prescribed prosthetic knees and the active knee prosthesis.
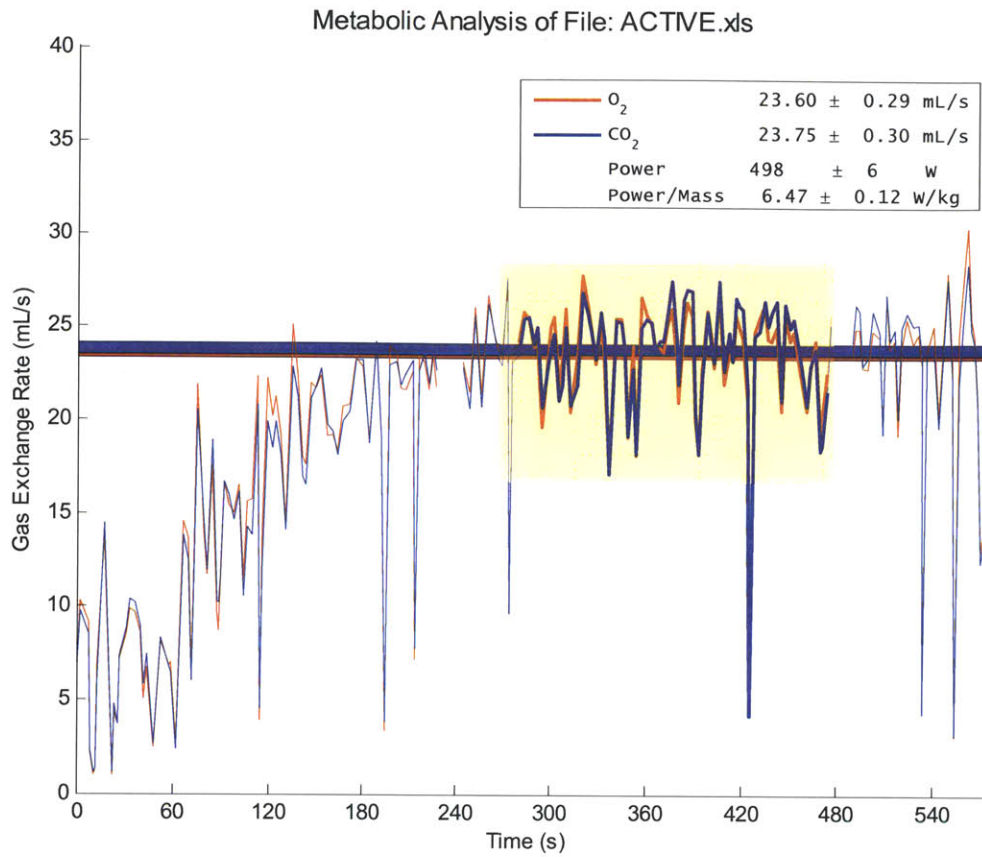
Figure 7.1 Example of gas exchange rate during walking at self-selected speed for calculating metabolic cost. Highlighted zone represents four minutes of steady-state walking.

	Prosthetic component mass [kg]		
Subject	Prescribed knee (incl. adaptors)	Active knee (incl. adaptors)	Ankle+foot (incl. shoe)
1	1.73	3.30	1.02
2	1.47	3.28	1.17
3	1.59	3.33	1.18
4	1.60	3.35	1.20

Table 7.3. Prosthetic system weight distribution

Results in walking speed and metabolic cost reduction for this study are in support of the initial hypotheses. For these results, it is important to consider the fact that the active knee prosthesis (including pylon and standard adaptors) is twice as heavy as each of the prescribed knee technologies in the study. The reduction and overall optimization for weight in the active knee can be an opportunity to improve the associated metabolic costs of walking for further studies. In addition, weight reduction strategies can allow for lighter amputees to wear the active knee and can also allow for the integration of powered foot-ankle prosthetic technologies.

7.3 Joint kinematics and kinetics

Pathologic gait in patients that have undergone an amputation results in higher energy consumption than a normal gait. In order to reduce energy consumption during walking, patients adopt different kinds of strategies and abnormal movements to compensate for the inefficiencies of their gait and to minimize energy usage. In search for the mechanisms that could explain the observed metabolic advantages of the active knee prosthesis as compared to conventional prescribed systems, we measured joint kinematics and kinetics of the study participants. The analysis was performed for the first three subjects. Corrupted force plate data for subject #4 produced unrealistic inverse dynamics calculations, and hence, they are not reported in this thesis.

The results indicate individual differences in the adaptive strategies incorporated by each amputee in order to guarantee a smoother and better coordinated gait pattern. Results for knee mechanics for the three subjects are presented in this chapter. The *affected* trajectories represent the prosthesis behavior. The mechanics of the active and prescribed prosthesis are depicted in red and blue, respectively. The unaffected (contralateral intact knee joint) mechanics are represented in black. Shaded regions for each trajectory represent the area within one standard deviation from the mean. Intact ankle biomechanics when using both types of prostheses did not reflect any significant differences throughout the gait cycle and are not shown in this chapter. The rest of the kinematic and kinetic results for hip and ankle for each of the subjects are included in the appendix as reference.

One of the major concerns of a transfemoral amputee is the prevention of knee buckling. The subjects in this investigation have modified affected knee biomechanics to provide additional stability. In particular, knee flexion during the first 40% of stance phase was very limited and/or non-existent when walking on both types of prostheses (conventional and active). These results were obtained despite the efforts of the certified prosthetist and author to promote stance knee flexion by posterior alignment of the patient's loading reference line with respect to active knee rotation center. This reference line bisects the lateral wall of the socket and was aligned posterior to the active knee center (0-5mm) to promote knee flexion. Alignment with the prescribed system remained unchanged throughout the testing period.
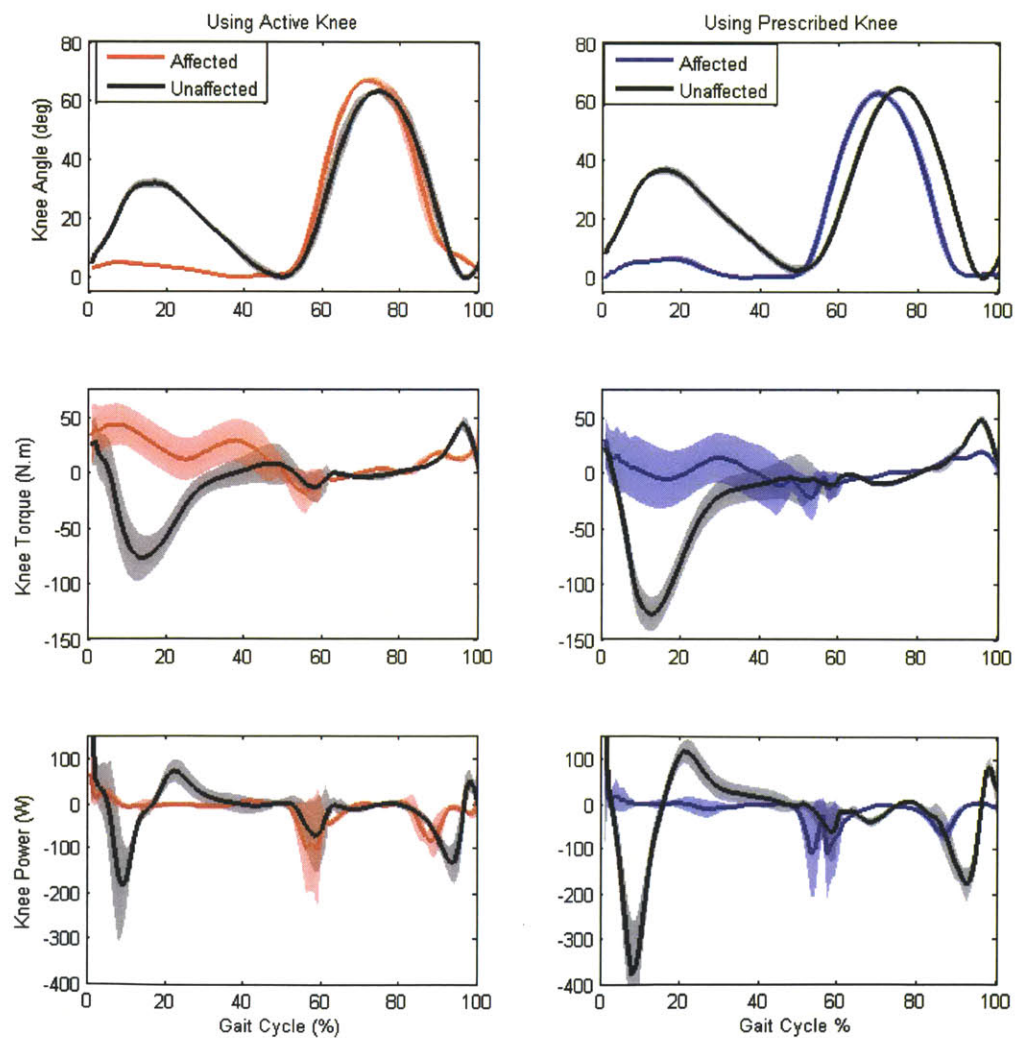
Figure 7.2 Knee joint biomechanics for subject 1

81

Inspection of active knee joint kinematics after pre-swing (through the rest of swing phase) shows certain improvements in gait symmetry over the conventional prescribed systems. This symmetry is observed when comparing knee flexion angle as well as swing phase duration. These results are more evident for subjects #1 and #2 than they are for subject #3.
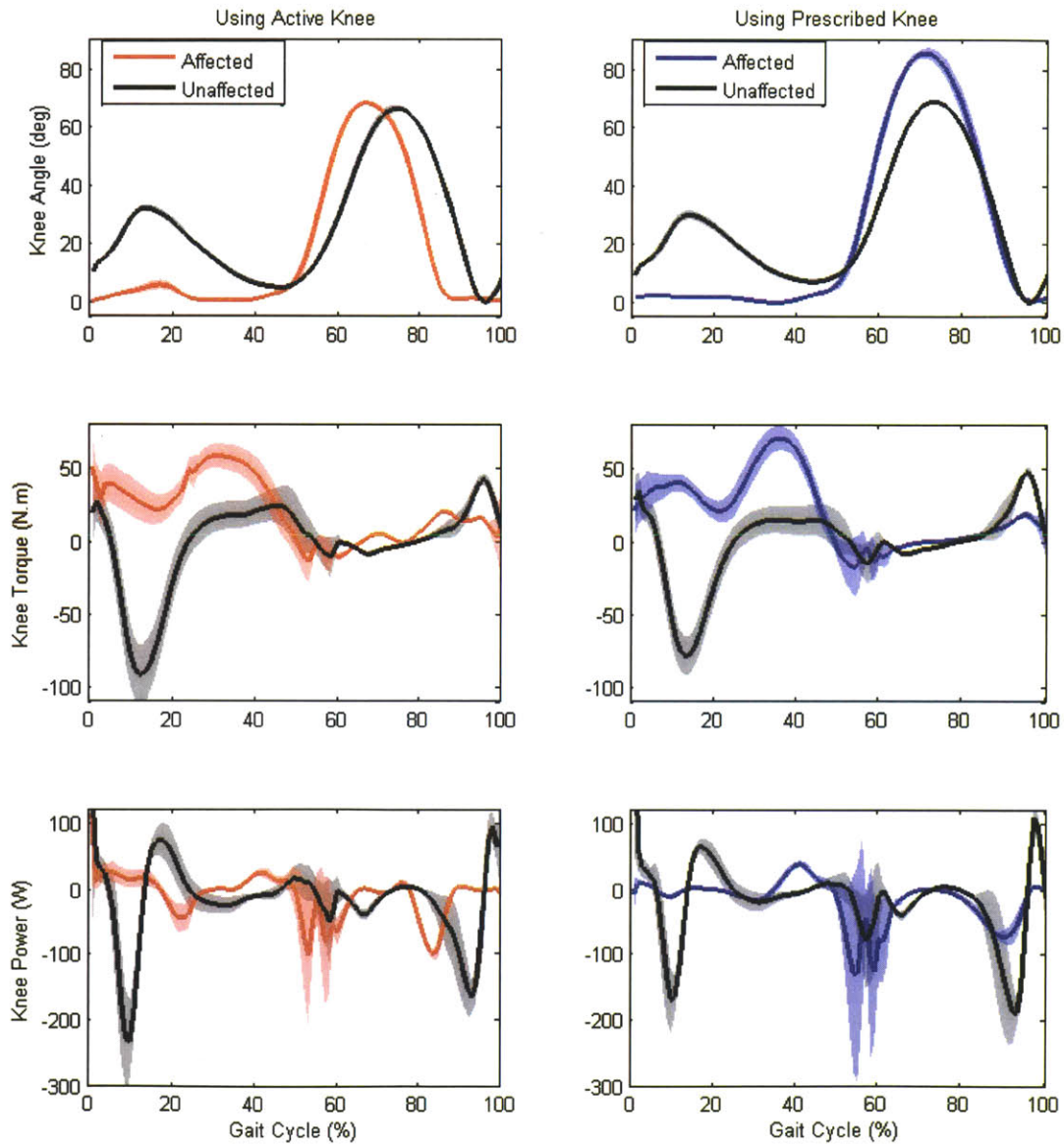

Figure 7.3 Knee joint biomechanics for subject 2

Due to the lack of early knee flexion during stance phase, prosthetic torque profiles during stance phase (for the active and prescribed knees) remain pathological as compared to the unaffected knee joint. Swing phase torque abnormalities are limited, the most predominant one being the lack of sufficient flexion torque at the end of swing to promote leg retraction right before heel strike. Such gait deviation is present across all three subjects when walking with their prescribed knees as well as with the active knee prosthesis.
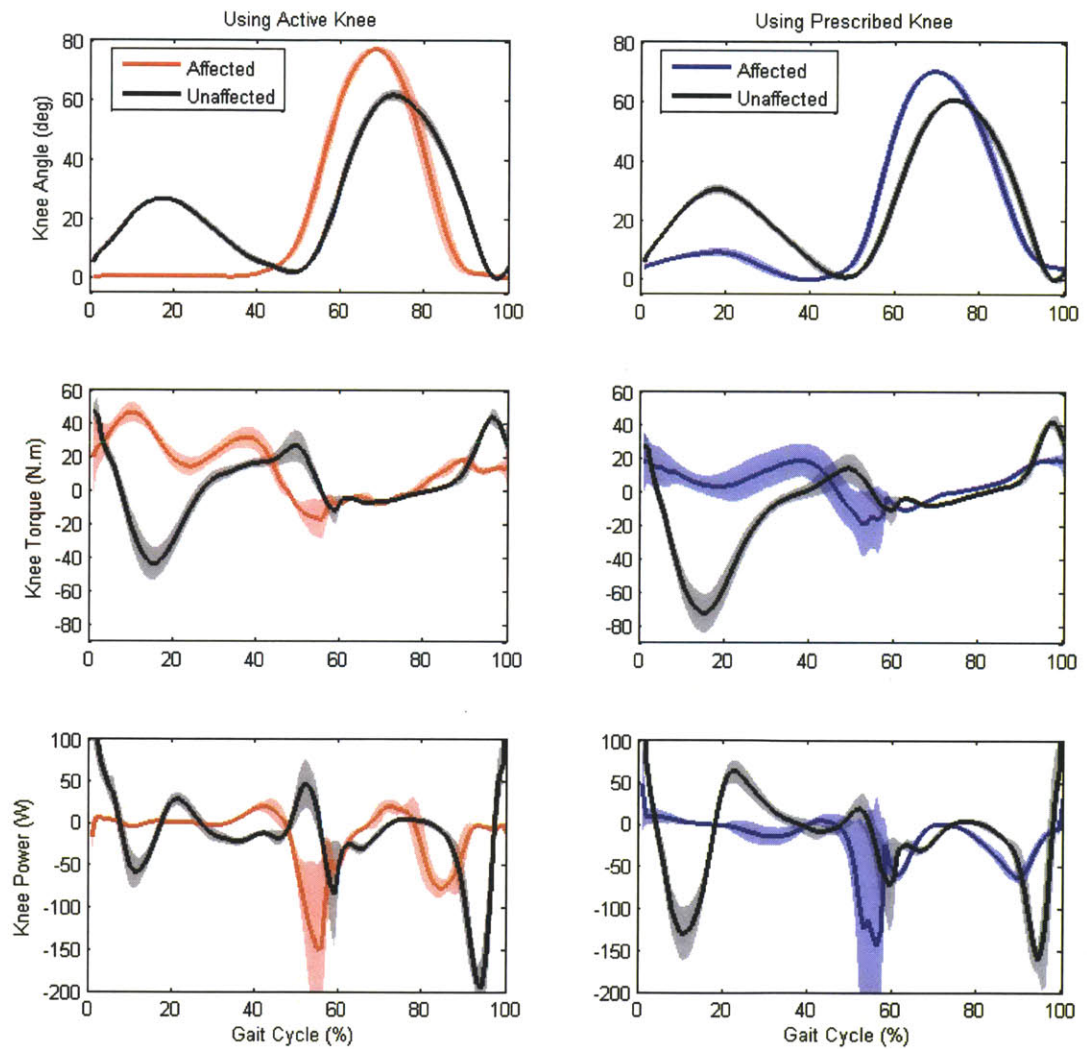

Figure 7.4- Knee joint biomechanics for subject 3

For the patients wearing the variable-damping knees (subjects #1 and #3), the unaffected knee torque when using the prescribed knees showed a large increase in peak extension torque during stance as compared to the unaffected knee torque while using the active knee prosthesis. For subject 2 (using a conventional hydraulic knee), the result is the opposite, with the torque for the unaffected side is greater when wearing the active knee than when wearing the prescribed system. This difference in unaffected loading response strategies of the intact (unaffected) knee joint among the three subjects may be influenced by the adaptation/training time required to adjust to the powered prosthesis. This effect should be further investigated with a larger subject population that can wear the different technologies with prolonged adaptation time for data collection.

When investigating hip biomechanics, we observe no significant differences in biomechanic behavior that can lead to metabolic advantages when using the active knee prosthesis as compared to the conventional prescribed systems. Results from published literature have compared hip behavior when using variable-damping prosthesis and mechanically passive devices (Johansson, et al. 2005). In that comparison, variable-damping knees were found to reduce hip work production, lower peak hip flexion at terminal stance, and reduce peak hip power generation at toe-off. At the beginning of the study presented in this thesis, we hypothesized that the active knee would further improve such parameters; however, results do not suggest any significant differences in hip biomechanics as a result of wearing the active knee versus any of the prescribed knees tested in the investigation.

The biomechanic results in this thesis are indicative of individual adaptation strategies by which our subjects have tried to minimize energetic cost consumption. A larger clinical study will be performed in order to provide statistical evidence for, and help discover the underlying mechanisms resulting in, the improvement of energetic cost which we observed in this study.

7.4 Knee damping in swing extension

We hypothesized that a variable-damping controller during swing extension improved knee mechanics during this phase. We quantified the swing extension damping profile of the

active knee prosthesis and compared it to the prescribed knee damping coefficient. Results for each of the subjects are depicted in the following figure. Red represents the prosthetic knee joints, and green represents the unaffected contralateral joint. Shaded regions represent one standard deviation from the mean. For the three subjects, the active knee's average swing extension damping coefficient trajectory better emulates the damping behavior of the unaffected knee joint.
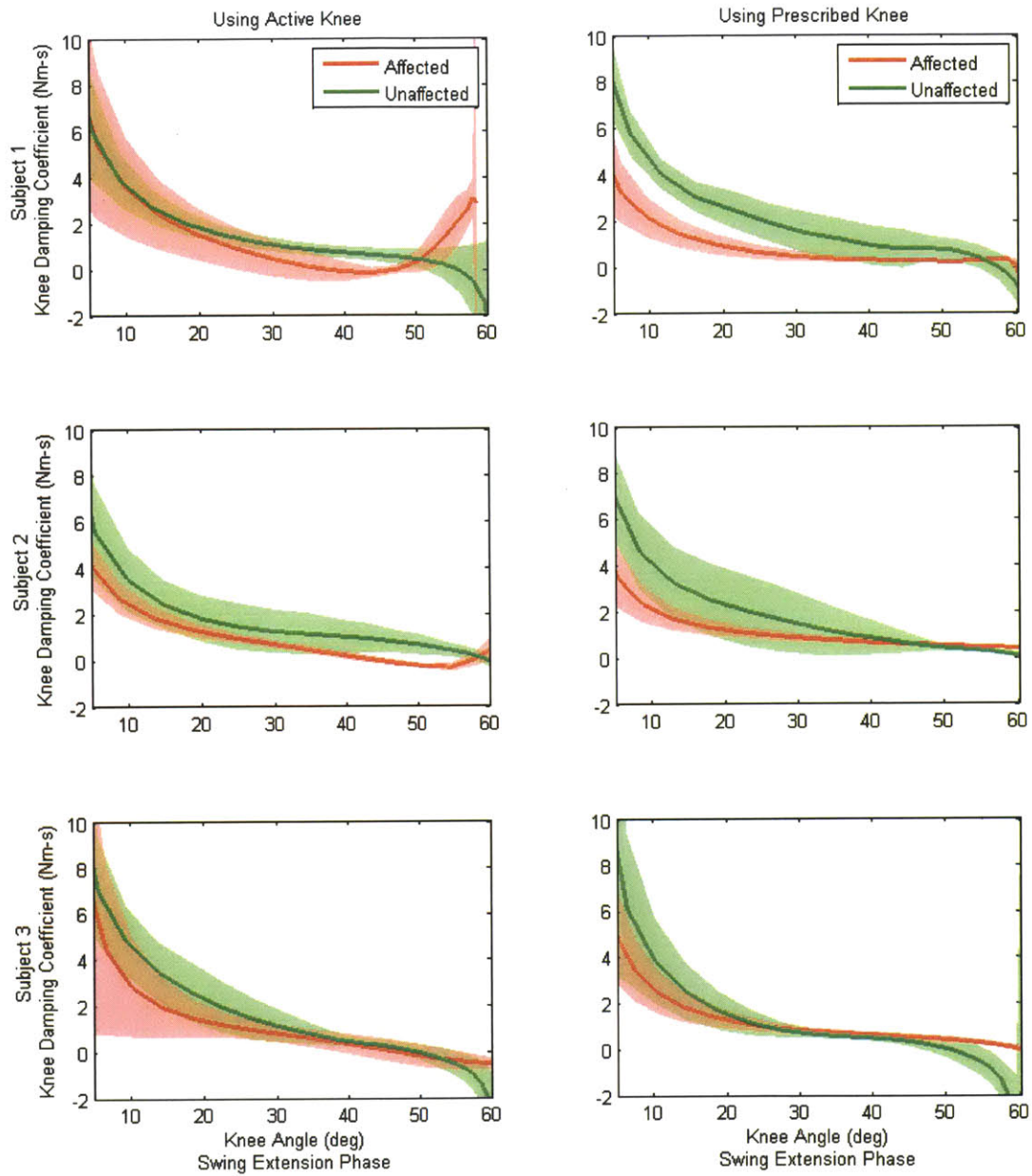
Figure 7.5 -Knee damping coefficient during swing extension phase for each of the three subjects.

To analyze the damping behavior symmetry, the root-mean-square (RMS) error between the of the unaffected and affected knee joints for swing phase was evaluated. It is assumed that normal gait is symmetrical and that deviation from a biological pattern is a sign of disability.

$$RMSE = \sqrt{\frac{1}{N}\sum \left(B(i)_{prosthesis} - B(i)_{unaffected}\right)^2}$$

where N represents the total number of samples in the data during swing extension phase. $B(i)_{prosthesis}$ and $B(i)_{unaffected}$ represent the damping coefficient during swing extension for the prosthesis and the intact knee joint, respectively.. Larger RMS error values represent a less symmetric damping profile between the prosthesis the the unaffected knee joint.

| Subject | Swing Extension RMS Error Knee Damping Coefficient (Nm.s) | |
	Using the active knee	Using the prescribed knee
1	0.86	1.63
2	0.89	1.20
3	0.88	1.06

Table 7.4. RMS Error for knee damping coefficient during swing extension phase using the active and prescribed knee prostheses.

In support of these results, transfemoral amputees in the study commented on the "smoothness" they perceived during swing phase when wearing the active knee prosthesis despite the added distal inertia. The amputees' subjective perception of the swing was that it was more "biological" and/or had a more "natural' feel.

7.5 Upper body vertical displacement

One of the most common abnormalities that subjects with transfemoral amputations present is ipsilateral upper body/ trunk bending during stance. This abnormal downward movement of the trunk over the prosthesis is a compensation mechanism to enhance stability. Moreover, this bending increases center of mass displacement of the gait cycle which is correlated with increments in metabolic cost.

We measured the amplitude of the vertical motion of the upper body (trunk) displacement during the complete gait cycle. This measurement was derived from the spatial motion data of the sacrum marker. The vertical amplitude of this displacement has been used by researchers as a close approximation of the vertical displacement of the body's center of mass in walking. Center of mass displacement has been previously correlated with energetic expenditure during walking, associating larger displacements with increases in metabolic cost. Figure 7.6 shows the vertical displacement of the trunk derived from sacrum spatial displacement for all subjects in the investigation.
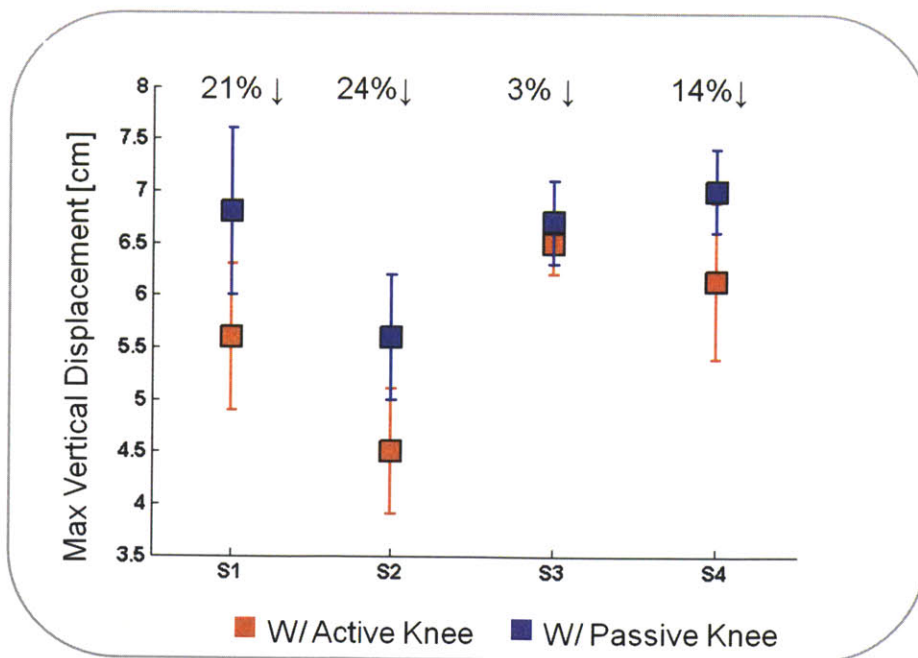

Figure 7.6 Vertical displacement of the trunk

The four subjects in the study showed a reduction in upper body vertical displacement (as measured by sacrum marker spatial displacement). On average, healthy intact persons exhibit approximately 2.3 cm vertical displacement of the center of gravity (Kishner 2011). These results may suggest that the use of the active knee prosthesis reduces the downward motion of the upper body, and this can contribute to the strategies for minimizing energy consumption during ambulation.

7.6 Concluding remarks and future work

The work presented in this thesis seeks to advance the development of viable active knee prostheses capable of improving amputee locomotion. In particular, a novel electromechanical design with a variable-impedance control strategy was developed in order to improve the metabolic cost of walking of transfemoral amputees walking at self-selected speeds. In contrast to current approaches to the design of powered knee prostheses, which have focused mainly on the use of single-motor transmission systems directly coupled to the knee joint, the active knee in this investigation has a novel design motivated on a variable-impedance prosthetic knee model comprised of two series elastic clutch mechanisms and a variable damper. Furthermore, the features for the design and implementation of the biomimetic active knee prosthesis were modeled after intact human-like weight, size and dynamic properties.

In comparison to single-motor and direct-drive powered prostheses, the biomimetic design and implementation of the active knee prosthesis is based on a mono-articular variable-impedance model. The electromechanical architecture of the active knee is comprised of two series elastic actuators positioned in parallel in an agonist-antagonist configuration. Because of its architecture, this knee can have a passive spring-like behavior with independently clutchable series-elastic elements during stance phase, and can also behave as a variable-damper during the swing phase of walking. This variable-impedance control strategy results in an energetically economical prosthetic system for level-ground locomotion, where the prostheses actuators do not perform positive work on the knee joint during level-ground walking. On the contrary, conventional direct-drive systems require high-electrical power consumption to emulate fully the

mechanical behavior of the human knee joint. Moreover, these types of single-motor transmission systems have not shown to provide a metabolic advantage to amputees during level-ground walking compared to conventional mechanically passive and variable-damping knee technologies.

It is important to note that since the knee design is fully motorized and has series-elastic force sensing, knee joint torque can be directly controlled for more energetically expensive tasks such as overcoming stair and ramp ascent as well as seating-standing maneuvers, among others. In summary, the knee design takes advantage of series elastic energy storage and return mechanisms in addition to leveraging the passive dynamics of the leg with variable impedance control.

The results of the preliminary clinical investigation suggest that the biomimetic active knee prosthesis with variable-impedance control can offer an improvement in the metabolic cost of walking at self-selected speeds over conventional (mechanically passive and variable-damping) knee prostheses. When using the active knee, subjects showed an increase in self-selected walking speed on level-ground, compared to when they used their prescribed systems. This speed increase remained within 5% of the selected speed when using their conventional prostheses. Moreover, a reduction in vertical displacement of the upper body was observed on all four participants. The decrease in vertical displacement of the trunk can be associated with a smoother gait, reducing center of gravity oscillations and improving metabolic energy expenditure during locomotion.

Based on the clinical results of this thesis, a future investigation with transfemoral amputees is proposed. This investigation should contemplate a comprehensive clinical study involving ten above knee amputees and intact human subjects that match the age, weight and height of the patients. This future study should include the measurement of metabolic, kinematic/kinetic and electromyographic data at three different walking speeds that cover slow, moderate and fast cadences. Such a study would allow for a deeper quantifiable understanding of the clinical impact of the biomimetic active knee prostheses, and could reveal the relevant

clinical differences that, we anticipate, would help explain the biomechanical and physiological mechanisms that result in a metabolic cost reduction.

In addition to a more comprehensive clinical evaluation, future research efforts towards the improvement of the design of the biomimetic active knee prosthesis should be considered. Some of the main areas of improvement include the revision of actuator and battery technologies, weight/dimension optimization, and the development of more sophisticated control strategies that promote customizable tuning to patients' gait needs.

With the work presented in this thesis, the author has sought to contribute to the development of integral assistive and rehabilitation technologies that can adapt to the needs of the physically challenged and, thus, improve their quality of life. Consequently, this work has sought to advance the field of Biomechatronics, helping lead to a better understanding of human-machine integration mechanisms that enhance human capabilities.

Bibliography

Au, S. (2007). *Powered ankle-foot prosthesis for the improvement of amputee walking economy.* Cambridge, MA. USA: MIT Ph.D. Thesis. Mechanical Engineering.

Au, S., & Herr, H. (2008). Powered Ankle-Foot Prosthesis. The importance of series and parallel motor elasticity. *IEEE Robotics and Automation Magazine*, 52-59.

Au, S., Martinez-Villalpando, E. C., & Herr, H. (2007). Powered Ankle-Foot Prosthesis for the Improvement of Amputee Ambulation. *IEEE Engineering in Medicine and Biology Conference* (pp. 3020-3026). Lyon: IEEE.

Au, S., Weber, J., & Herr, H. (2009). Powered ankle-foot prosthesis improves walking metabolic economy. *IEEE Transactions on Robotics, 25*, 51-66.

Blaya, J. A., & Herr, H. (2004). Adaptive control of a variable-impedance ankle-foot orthosis to assist drop-foot gait. *IEEE Transactions on Neural Systems and Rehabilitation Engineering, 12*(1), 24-31.

Brockway, J. M. (1987). Derivation of formulate used to calculate energy expenditure in man. *Human Nutition: Clinical Nutrition, 41*, 463-471.

Collins, S. H., & Kuo, A. D. (2010). Recycling energy to restore impaired ankle function during human walking. *PLoS ONE, 5*(2), e9307.

Durkin, L. J., & Dowling, J. J. (2006). Body Segment Estimation of the Human Lower Leg Using an Elliptical Model with Validation from DEXA. *Annals of Biomedical Engineering*, 1483-1493.

Elliott, G. (2012). *Design and evaluation of a quasi-passive robotic knee brace: on the effects of parallel elasticity on human running.* Cambridge, MA: Massachusetts Institute of Technology. Ph.D. Thesis. Department of Electrical Engineering and Computer Science.

Endo, K., Paluska, D., & Herr, H. (2006). A quasi-passive model of human leg function in level-ground walking. *IEEE/RSJ International Conference on Intelligent Robots and Systems (IROS)*, (pp. 4935-4939). Beijing, China.

Feinglass, J., Brown, J. L., LaSasso, A., Sohn, M. W., Manheim, L. M., Shah, S. J., et al. (1999, August). Rates of lower-extremity amputation and arterial reconstruction in the United States, 1979 to 1996. *American Journal of Public Health, 89*(8), 1222-1227.

Fite, K., Mitchell, J., & Goldfarb, M. (2007). Design and control of an electrically powered knee prosthesis. *IEEE 10th International Conference on Rehabilitation Robotics (ICORR)*, (pp. 902-905).

Flowers, W. (1972). A man-interactive simulator system for above-knee prosthetics studies. *Ph.D. Thesis*. Cambridge, MA: Massachusetts of Institute Technology, Department of Mechanical Engineering.

Gates, D. (2004). Characterizing the ankle function during stair ascent, descent and level walking for ankle prosthesis and orthosis design. *Master's thesis*. Boston, MA: Boston University.

Grimes, D. (1979). An active multimode above knee prosthesis controller. *Ph.D. thesis*. Cambridge, MA: Massachusetts Institute of Technology, Department of Mechanical Engineering.

Herbert, L. M., Engsberg, J. R., Tedford, K. G., & Grimston, S. K. (1994, October). A comparison of oxygen consumption during walking between children with and without below-knee amputations. *Physical Therapy, 74*, 943-950.

Herr, H., & Popovic, M. (2008). Angular Momentum in Human Walking. *Journal of Experimental Biology*(211), 467-481.

Herr, H., & Wilkenfeld, A. (2003). User-adaptive control of a magnetorheological prosthetic knee. *Industrial Robot, An International Journal, 30*, 42-55.

Hitt, J., Bellman, R., Holgate, M., Sugar, T., & Hollander, K. (2006). The sparky (spring ankle with regenerative kinetics) projects: Design and analysis of a robotic transtibial prosthesis with regenerative kinetics. *Proceedings of the IEEE International Conference on Robotics and Automation*, (pp. 2939-2945).

Hogan, N. (1985). Impedance contorl: an approach to manipulation: Part I-III. *ASME Journal of Dynamic Systems, Measurement and Control, 107*, 1-24.

Huang, G. F., Chou, Y. L., & Su, F. C. (2000). Gait analysis and energy consumption of below-knee amputees wearing three different prosthetic feet. *Gait & Posture, 12*, 162-8.

James, U. (1973). Oxygen uptake and heart rate during prosthetic walking in healthy male unilateral above-knee amputees. *Scandinavian Journal of Rehabilitation Medicine, 5*, 71-80.

Johansson, J., Sherrill, D., Riley, P., & Paolo, B. H. (2005). A clinical comparison of variable-damping and mechanically-passive prosthetic knee devices. *American Journal of Physical Medicine & Rehabilitation, 84*(8), 563-575.

Kadaba, M., Ramakrishnan, H., & Wootten, M. (1990). Measurement of lower extremity kinematics during level walking. *Journal of Orthopedic Research, 8*(3), 383-392.

Kapti, A., & Yucenur, M. S. (2006). Design and control of an active artificial knee joint. *Mechanism and Machine Theory, 41*, 1477-1485.

Kitayama, I., Nakagawa, N., & Amemori, K. (1992). A microcomputer controlled intelligent A/K prosthesis. *Proceedings of the 7th World Congress of the International Society for Prosthetics and Orthotics.* Chicago.

Koganezawa, K., & Kato, I. (1987). Control aspects of artificial leg. In M. Nalecz (Ed.), *IFAC Control Aspects of Biomedical Engineering* (pp. 71-85). Oxford: Pergamon Press.

Koniuk, W. (2001, March 23). *Patent No. 6443993.* United States of America.

Lehmann, J. F., Price, R., Boswell-Bessette, S., Dralle, A., & Questad, K. (1993). Comprehensive analysis of dynamic elastic response feet: Seattle Ankle/Lite Foot versus SACH foot. *Archives of Physical Medicine and Rehabilitation, 74*, 853-861.

Martinez-Villalpando, E.C.; Weber, J.; Elliott, G.; Herr, H. (2008). "Design of an agonist-antagonist active knee prosthesis," *Biomedical Robotics and Biomechatronics, BioRob 2nd IEEE RAS & EMBS International Conference,* pp.529-534, Oct. 19-22

Martinez-Villalpando, E. C., Weber, J., Elliott, G., and Herr, H. (2008). Biomimetic Prosthetic Knee Using Antagonistic Muscle-Like Activation. , *ASME International Mechanical Engineering Congress and Exposition (IMECE)*, Boston, MA., pp. 141-143, Oct. 31–Nov. 6.

Martinez-Villalpando, E. C., and Herr, H.(2009). "Agonist-Antagonist Active Knee Prosthesis: A Preliminary Study in Level Ground Walking." *Journal of Rehabilitation Research & Development (JRRD)* 46(3): 361-73.

Martinez-Villalpando, E.C.; Mooney, L.; Elliott, G.; Herr, H. (2011). "Antagonistic active knee prosthesis. A metabolic cost of walking comparison with a variable-damping prosthetic knee," *IEEE Engineering in Medicine and Biology Society, EMBC,* pp.8519-8522, Aug. 30 -Sept. 3.

McGeer, T. (1990). Passive Dynamic Walking. *International Journal of Robotics.*

Molen, N. H. (1973). Energy-speed relation of below-knee amputees walking on a motor-driven treadmill. *Internationale Zeitschrift für Angewandte Physiologie, 31*, 173-185.

Mooney, L. (2012). A variable-damping controler for a prosthetic knee during swing extension. Cambridge, MA: Massachusetts Institute of Technology. Bachelor of Science Thesis. Department of Mechanical Engineering.

National Limb Loss Information Center. (2008, September 18). *Amputation statistics by cause: Limb loss in the United States.* Retrieved March 16, 2012, from Amputee Coalition: http://www.amputee-coalition.org/fact_sheets/amp_stats_cause.html

Palmer, M. (2002). Sagittal plane characterization of normal human ankle function across a range of walking gait speeds. *Master's thesis*. Cambridge, MA: Massachusetts Institute of Technology.

Perry, J. (1992). *Gait analysis: Normal and pathological function*. Thorofare, NJ: Slack, Inc.

Postema, K., Hermens, H. J., de Vries, J., Koopman, H. F., & Eisma, W. H. (1997). Energy storage and release of prosthetic feet. Part 1: Biomechanical analysis related to user benefits. *Prosthetics and Orthotics International, 21*, 17-27.

Pratt, G. A., & Williamson, M. M. (1995). Series elastic actuators. *Proceedings on IEEE/RSJ International Conference on Intelligent Robots and Systems*, (pp. 399-406). Pittsburgh, PA.

Radcliffe, C. W. (1977). The Knud Jansen lecture: Above knee prosthetics. *Prosthetics and Orthotics International, 1*, 146-160.

Riener, R., Rabuffetti, M., & Frigo, C. (2002). Stair Ascent and Descent at Different Incliniations. *Gait and Posture*, 32-44.

Rose, J., & Gamble, J. (2006). *Human Walking* (Third Edition ed.). Philadelphia, PA: Lippnicott Williams & Wilkins.

Stein, R. B., Rolf, R., James, K., & Tepavic, D. (1990). Active suspension above-knee prosthesis. *International Conference on Biomedical Engineering*. Singapore.

Stepien, J., Cavenett, S., Taylor, L., & Crotty, M. (2007). Activity levels among lower-limb amputees: Self-report versus step activity monitor. *Archives of Physical Medicine and Rehabilitation, 88*(7), 896-900.

Sup, F., Bohara, A., & Goldfarb, M. (2008). Design and control of a powered transfemoral prosthesis. *International Journal of Robotics Research, 27*(2), 263–273.

Sup, F., Varol, H. A., Mitchell, J., Withrow, T. J., & Goldfarb, M. (2009). Selfcontained powered knee and ankle prosthesis: Initial evaluation on a transfemoral amputee. *Proceedings of the IEEE 11th International Conference on Rehabilitation Robotics*, (pp. 638–644).

Thomas, S. S., Buckon, C. E., Helper, D., Turner, N., Moor, M., & Krajbich, J. I. (2000). Comparison of the Seattle Lite Foot and Genesis II Prosthetic Foot during walking and running. *Journal of Prosthetics and Orthotics, 12*, 9-14.

Tilley, A R; Henry Dreyffus Associates. (2002). *The Measure of Man & Woman. Human Factors in Design*. New York: John Wiley & Soncs INc.

Torburn, L., Perry, J., Ayyappa, E., & Shanfield, S. L. (1990). Below-knee amputee gait with dynamic elastic response prosthetic feet: a pilot study. *Journal of Rehabilitation Research and Development, 27,* 369-384.

Waters, R. L., & Mulroy, S. (1999). The energy expenditure of normal and pathologic gait. *Gait & Posture, 9,* 207-231.

Whittle, M. W. (1991). *Gait analysis: an introduction* (3rd ed.). Oxford: Butterworth-Heinemann.

Wilkenfeld, A. J. (2000). Biologically inspired auto adaptive control of a knee prosthesis. *Ph.D. thesis.* Cambridge, MA: Massachusetts Institute of Technology.

Winter, D. (1990). *Biomechanics and motor control of human movement.* New York (NY): Wiley.

Winter, D. A. (1983). Biomechanical motor pattern in normal walking. *Journal of Motor Behavior, 15*(4), 302-330.

Winter, D. A. (2005). *Biomechanics of Motion of Human Movement.* New York: John Wiley & Sons Inc. Third Edition.

Wisse, W. (2004). Essentials of dynamic walking: Analysis and design of two-legged robots. *PhD Thesis.* Delft, Netherlands: Technical University of Delft.

Zahedi, S. (1993). The results of the field trial of the Endolite Intelligent Prosthesis. *XII International Congress of INTERBOR.*

Ziegler-Graham, K. (2008). Estimating the prevalence of limb loss in the United States - 2005 to 2050. *Archives of Physical Medicine and Rehabilitation, 89,* 422-429.

Zlatnik, D., Steiner, B., & Schweitzer, G. (2002). Finite-state control of a trans-femoral prosthesis. *IEEE Transactions on Control System Technology, 10*(3), 408-420.
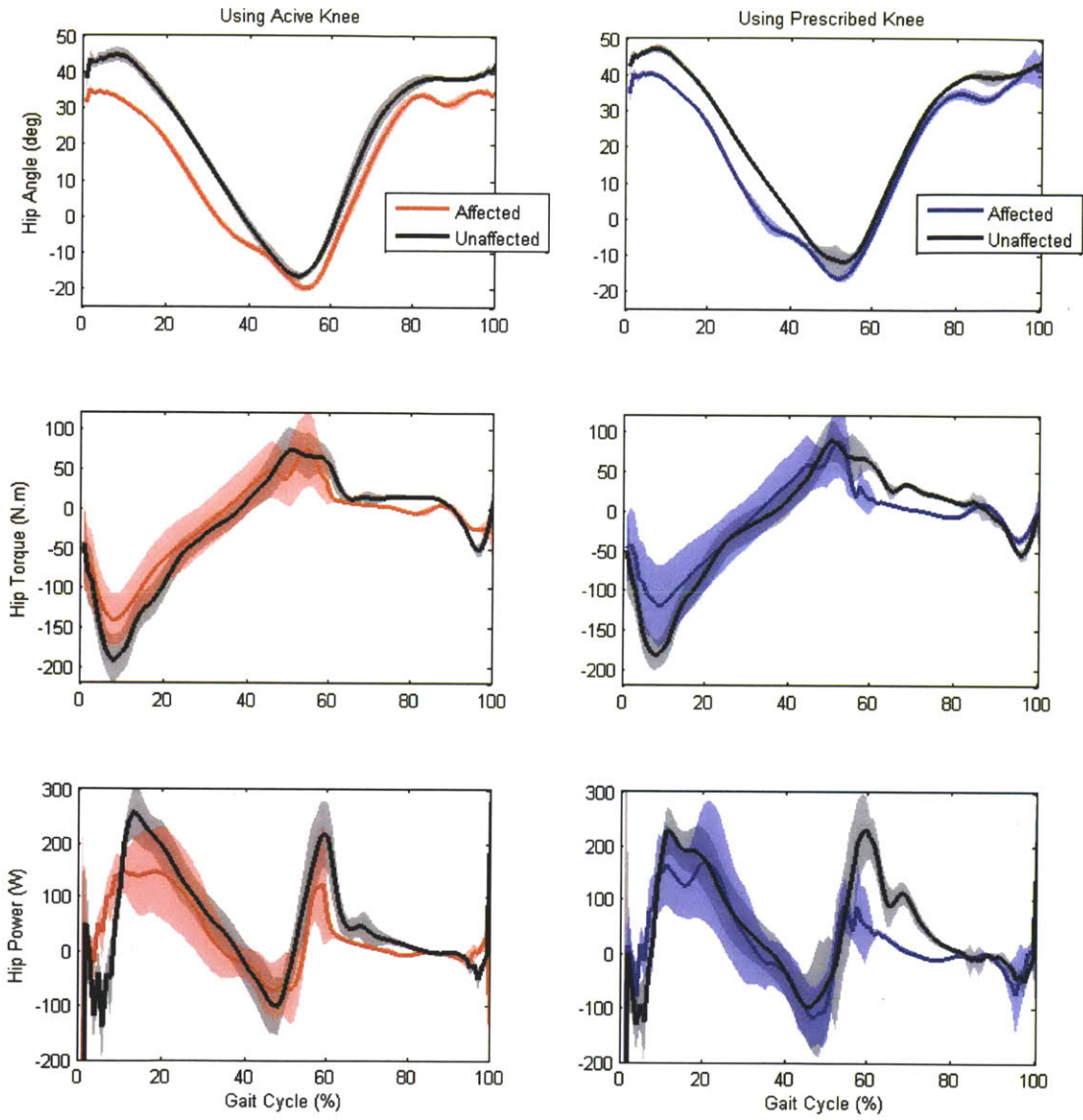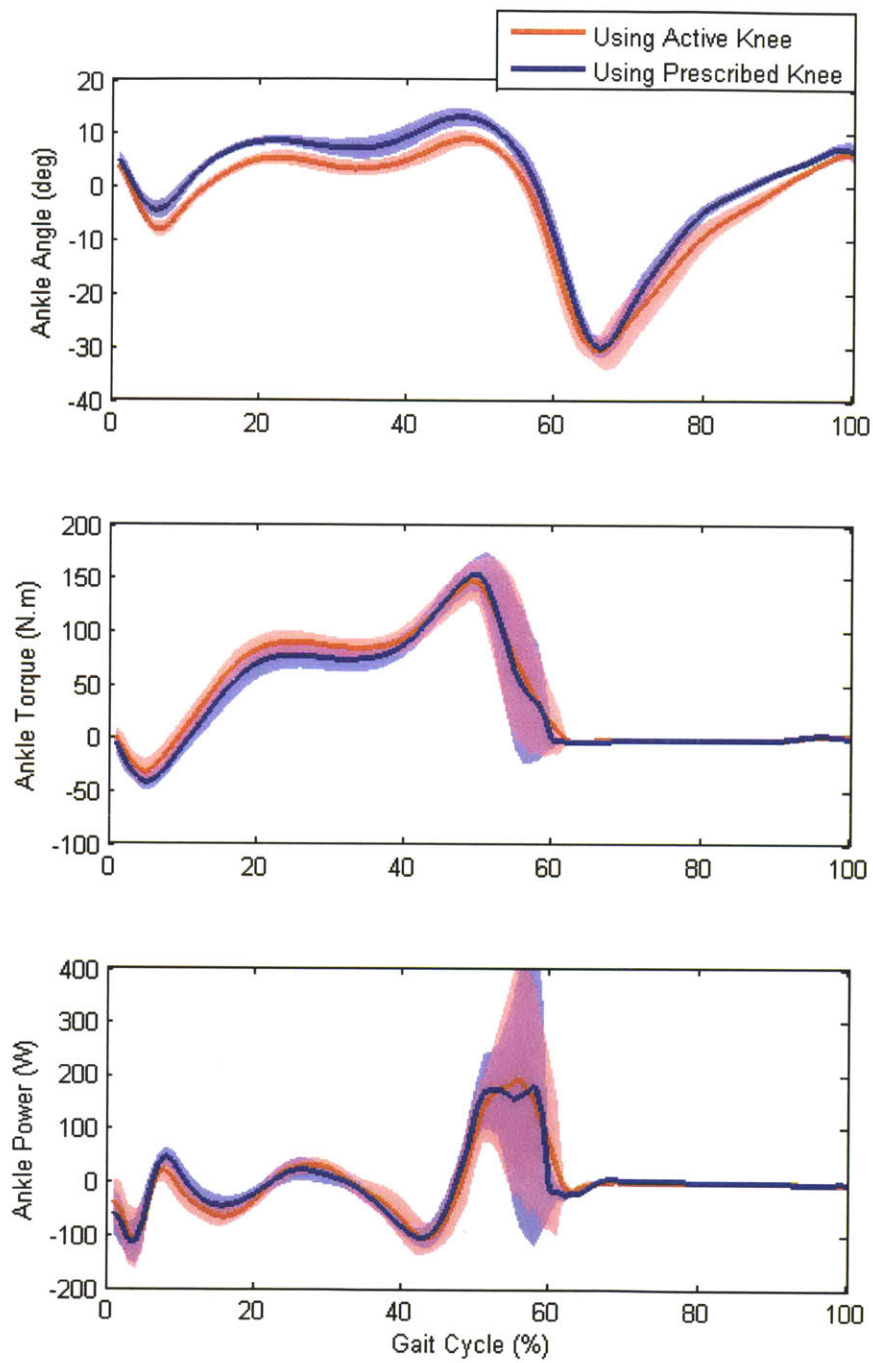
www.ossur.com.

www.iwalk-free.com

www.cosmed.it

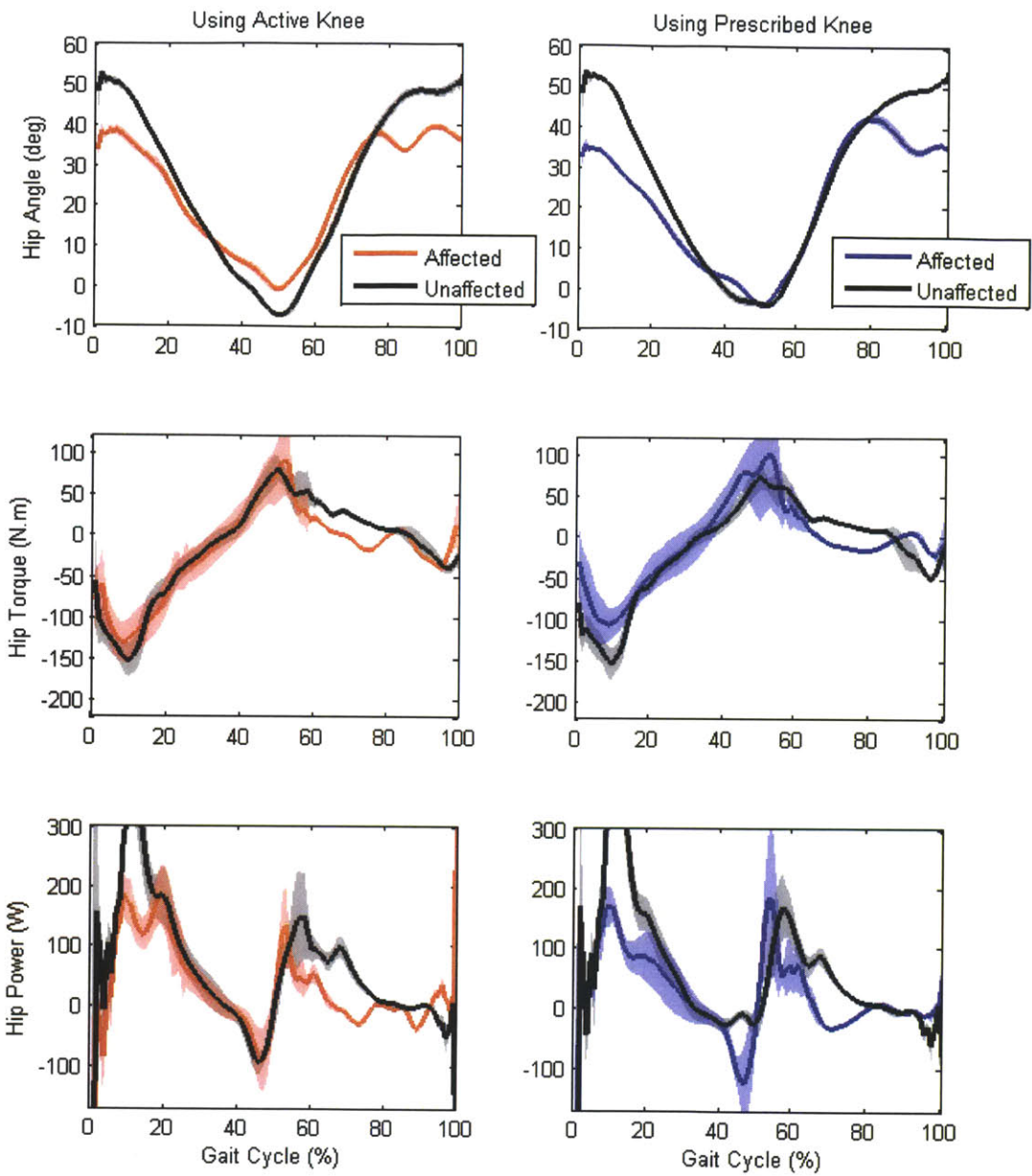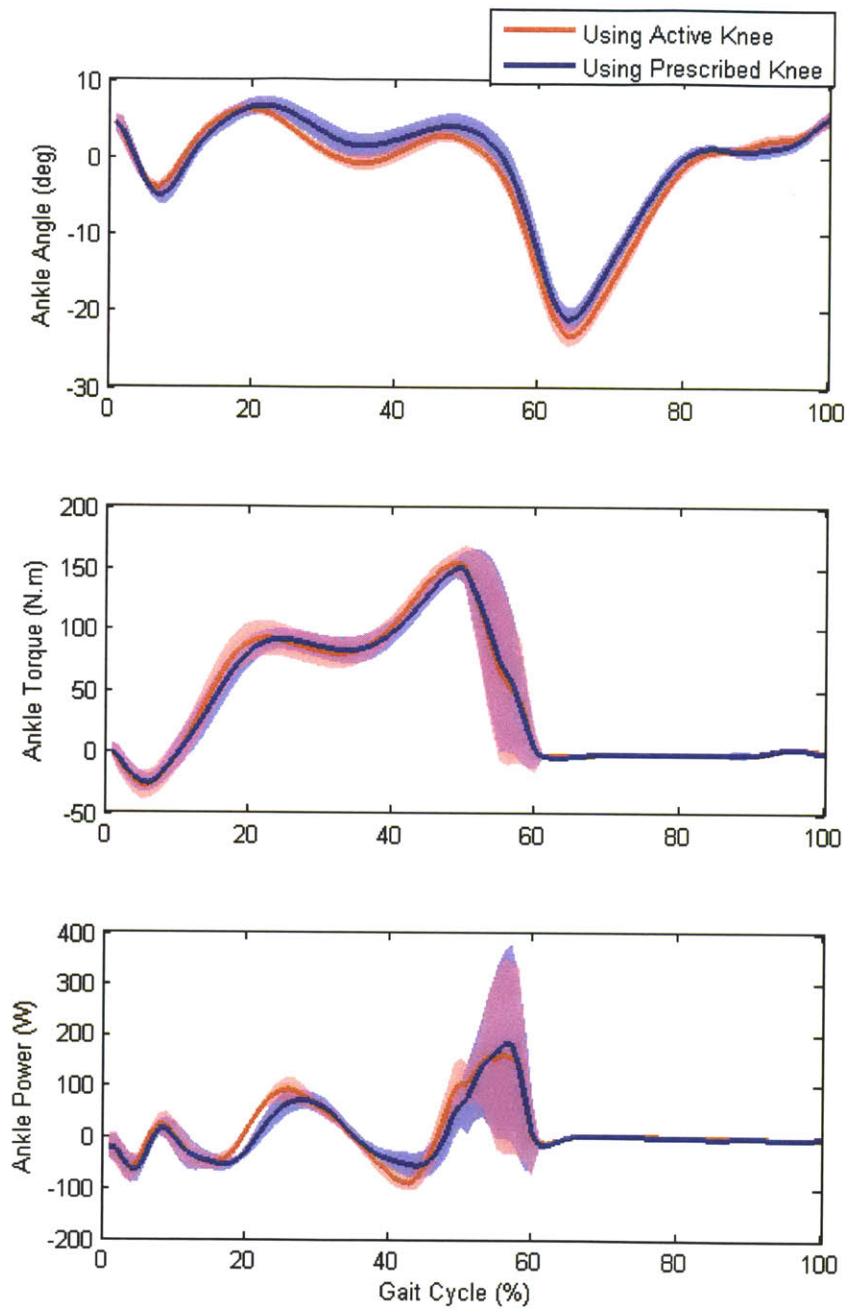www.vicon.com

www.musculographics.com
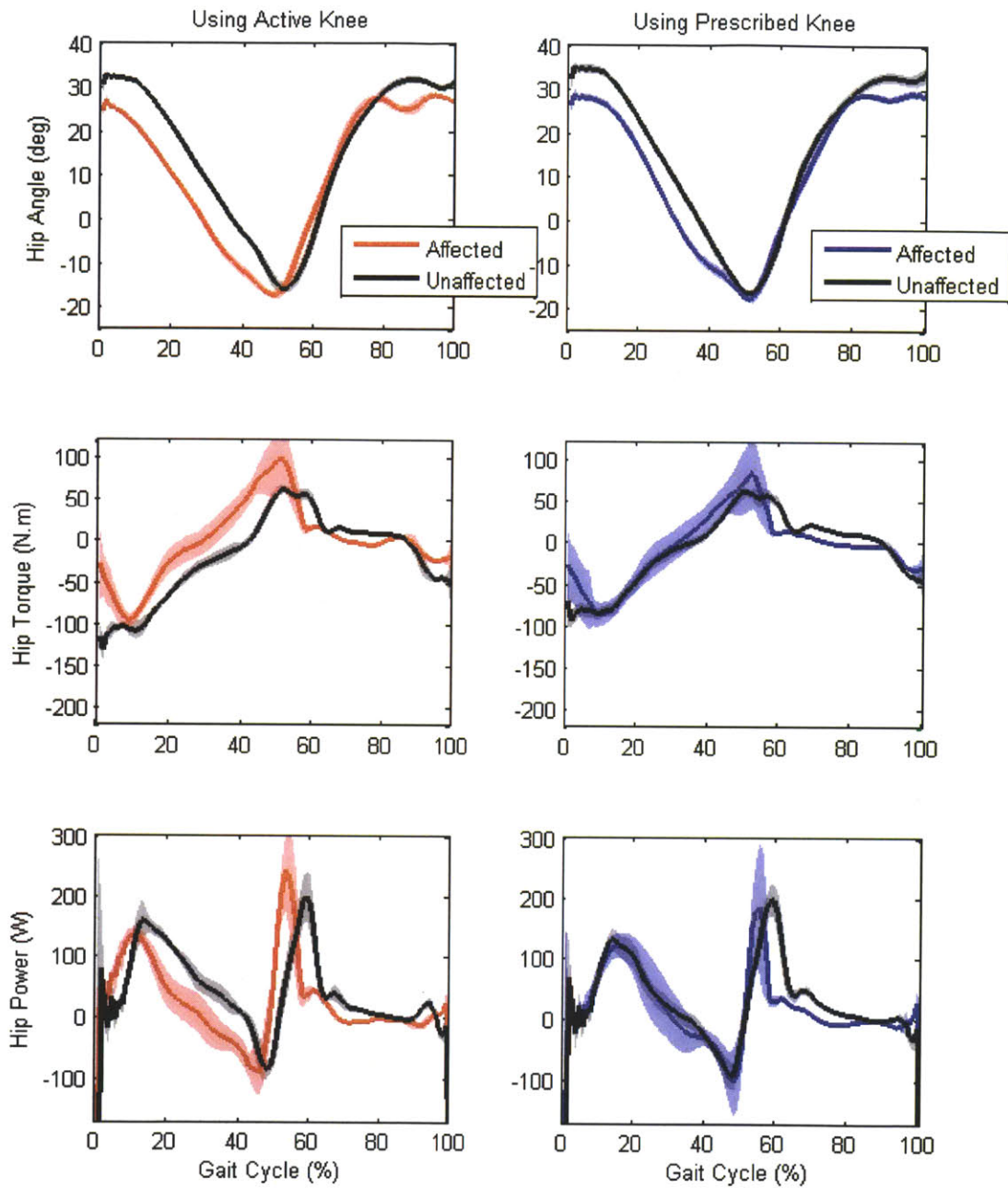
Appendix

A1. Hip biomechanics for subject 1

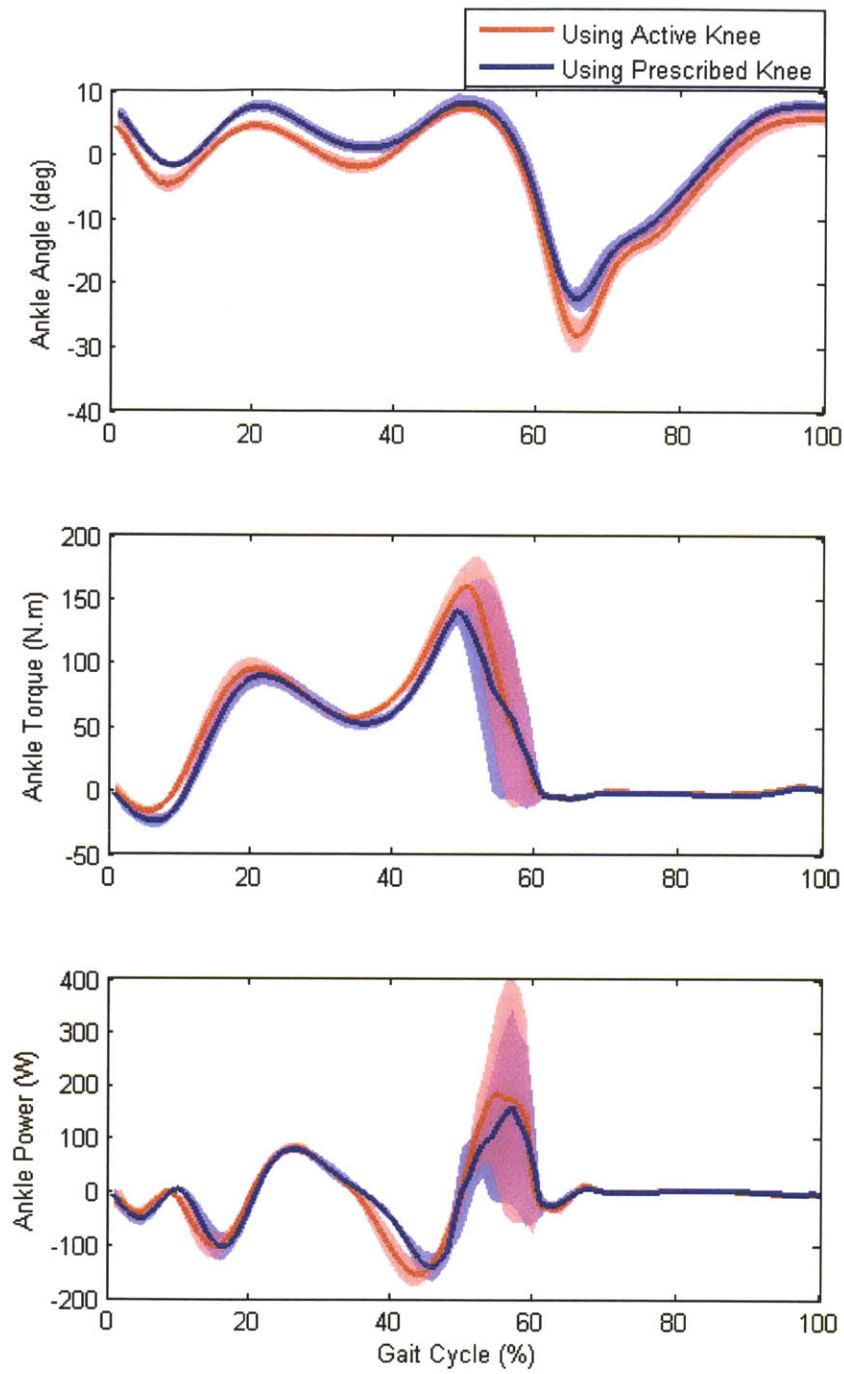A2. Unaffected ankle biomechanics for subject 1

A3. Hip biomechanics for subject 3

A4. Unaffected ankle biomechanics for subject 2

A5. Hip biomechanics for subject 3

A6. Ankle biomechanics for subject 3